A MATHEMATICAL MODEL OF FLARE PLUME COMBUSTION AND RADIATION

John E. Tanner, Jr.

Naval Weapons Support Center
Crane, Indiana

30 June 1975

DISCLAIMER NOTICE

THIS DOCUMENT IS BEST QUALITY PRACTICABLE. THE COPY FURNISHED TO DTIC CONTAINED A SIGNIFICANT NUMBER OF PAGES WHICH DO NOT REPRODUCE LEGIBLY.

NWSC/CR/RDTR-9

A MATHEMATICAL MODEL OF FLARE PLUME COMBUSTION AND RADIATION

by
John E. Tanner, Jr.

NAVAL WEAPONS SUPPORT CENTER
APPLIED SCIENCES DEPARTMENT
CRANE, INDIANA 47522

30 June 1975

FINAL REPORT for Period 1 July 1972 to 30 June 1974

Prepared for
Commander
NAVAL AIR SYSTEMS COMMAND
Washington, D. C. 20361

UNCLASSIFIED

SECURITY CLASSIFICATION OF THIS PAGE (When Data Entered)

REPORT DOCUMENTATION PAGE		READ INSTRUCTIONS BEFORE COMPLETING FORM
1. REPORT NUMBER NWSC/CR/RDTR-9	2. GOVT ACCESSION NO.	3. RECIPIENT'S CATALOG NUMBER
4. TITLE (and Subtitle) A MATHEMATICAL MODEL OF FLARE PLUME COMBUSTION AND RADIATION		5. TYPE OF REPORT & PERIOD COVERED Final Report 1 July 1972-30 June 1974
		6. PERFORMING ORG. REPORT NUMBER
7. AUTHOR(s) John E. Tanner, Jr.		8. CONTRACT OR GRANT NUMBER(s) AIRTASK A310310C/ 159A/4R02402002
9. PERFORMING ORGANIZATION NAME AND ADDRESS Naval Weapons Support Center Applied Sciences Department Crane, Indiana 47522		10. PROGRAM ELEMENT, PROJECT, TASK AREA & WORK UNIT NUMBERS 61153N, WR02402, WR02402002
11. CONTROLLING OFFICE NAME AND ADDRESS Naval Air Systems Command (Code Air-310C) Washington D.C. 20361		12. REPORT DATE 30 June 1975
		13. NUMBER OF PAGES 84
14. MONITORING AGENCY NAME & ADDRESS (if different from Controlling Office)		15. SECURITY CLASS. (of this report) UNCLASSIFIED
		15a. DECLASSIFICATION/DOWNGRADING SCHEDULE

16. DISTRIBUTION STATEMENT (of this Report)

APPROVED FOR PUBLIC RELEASE; DISTRIBUTION UNLIMITED

17. DISTRIBUTION STATEMENT (of the abstract entered in Block 20, if different from Report)

18. SUPPLEMENTARY NOTES

19. KEY WORDS (Continue on reverse side if necessary and identify by block number)

Pyrotechnics
Plume
Modeling
Combustion
Illuminating Flares

20. ABSTRACT (Continue on reverse side if necessary and identify by block number)

See Reverse

DD FORM 1 JAN 73 1473 EDITION OF 1 NOV 65 IS OBSOLETE
S/N 0102-014-6601 | i

UNCLASSIFIED

SECURITY CLASSIFICATION OF THIS PAGE (When Data Entered)

A mathematical model of combustion and radiation in the plume of a pyrotechnic flare is constructed based on observations and on relevant radiation and thermodynamic theory.

The model is applied to specific cases by means of computer program which computes the equilibrium thermodynamic properties and the radiation rates at closely spaced points from the flare surface, where combustion begins, to the tail of the plume where radiation is essentially zero. Tests against experimental data, using magnesium-fueled flares with a sodium-containing oxidizer show that predicted changes in luminous efficiency due to changes in oxidizer composition, fuel percent, pressure, and ambient oxygen content correlate moderately well with observations.

The calculations indicate that in real flares a significant amount of air augments combustion and that this air has a large effect on flame temperature and on luminous output. Maximum temperatures reached are probably within 200 degrees of computed adiabatic temperatures for all but extremely fuel-rich flares.

The smoke is found to emit as a weak graybody. Burning times for the magnesium particles are indicated to be considerably shorter than those predicted from single particle burning experiments.

When appropriate theoretical and experimental input data are supplied, the program should be useful for predicting output from new formulas giving radiation in a large number of wavelengths or wavelength bands. Specifically, the model should be useful for formulating colored flares and infrared flares.

SUMMARY

A thermodynamic model of combustion and radiation in the plume of a pyrotechnic flare has been constructed for the purpose of predicting radiant efficiencies of untried formulations.

Plume properties and flow are modeled in one dimension only--parallel to the axis of the plume. The plume composition is derived from the equilibration of the binder, oxidizer, admixed air, and a portion of the metal fuel particles. The vaporization of fuel is assumed to be the slow step in the reaction. Energy losses are assumed due to radiation only. Energy transfer along the axis of the plume by radiative or other mechanisms is ignored.

The starting point is taken in the gas phase just above the flare surface. All of the binder and oxidizer are assumed to have reacted, along with enough of the fuel (5-10%) to raise the adiabatic flame temperature to about 1000 K, in accord with experimentally deduced values.

Equilibrium temperatures and species concentrations are computed at closely-spaced points from the starting point, proceeding parallel to the plume axis, until well into the tail of the plume where temperatures have dropped to the point where the radiation of interest is essentially zero. Increments of air and of any remaining fuel are added to each point. Radiation losses for all of the important radiative processes and for the processes of interest are computed for the interval

between each pair of points and are subtracted from the enthalpy used in calculating equilibrium properties at the next point.

For a test of the model magnesium-fueled flares with a sodium-containing oxidizer and an organic binder were chosen. It was assumed that the most important radiative processes were sodium-D emission and graybody emission. A radiative transfer model in an optically dense medium was constructed for computing sodium-D emission. Graybody radiation was taken as proportional to the fourth power of the local temperature.

A computer program was obtained for performing the calculations by modifying a program in the literature.

There were a number of parameters whose values could not be determined *a priori*. These included the rates of air mixing and of fuel consumption, the absolute rates of radiation, and the plume spreading angle. The functional form of these quantities was deduced from theory or arbitrarily, and the absolute values were adjusted so as to give agreement with observations of plume shape, the point of maximum brightness, the total visible length, and the luminous efficiency for a limited set of observations.

Computations were then performed for a wide range of fuel/oxidizer ratios, oxidizer formulas, binder percentages, ambient pressures, and ambient compositions and compared with experimental values from the literature. Agreement

between computed and literature values of luminous efficiency varied from moderate to good.

Modifications were indicated by which the program can be used for formulas where other types of radiation are of interest. An example suggested is the calculation of the green radiation at 5200 Å from the $^2\Pi$ excited electronic state of the BaCl radical.

It was recommended that the necessary data be acquired and modifications made so that the program could be applied to colored flares or to infrared flares. It was also recommended that the model be refined (1) by a reoptimization of the arbitrary input parameters (rate of air mixing, etc.), (2) by modifying the fuel input (vaporization) to take account of local oxygen concentration, and (3) by including a consideration of the heat feedback parallel to the plume axis.

PREFACE

This work is part of a larger program directed at a better understanding of pyrotechnic flare combustion and radiation. Besides modeling, the program includes high resolution spectroscopy and band radiometry in the visible and infrared wavelengths.

Thanks are due to Drs. Harold Sabbagh, Henry Webster, Carl Dinerman, and John O'Benar of NWSC for helpful comments on the manuscript.

The typing and editing of this report by Miss Karla Harker is greatly appreciated.

TABLE OF CONTENTS

LIST OF FIGURES

TABLE OF CONTENTS (cont.)

LIST OF TABLES

INTRODUCTION

Many experimental and theoretical studies of the combustion of flares have been made to determine the details of the combustion and light emission processes so that a better understanding of their operation could point the way to devising flares of greater luminosity or color purity.[1-7] Modeling of related phenomena has also been done.[8]

The task of the present study has been to construct a theoretical model of flare combustion which would incorporate all the experimental observations and at the same time test them for consistency. The goal is to be able to predict radiant efficiency of new formulations at selected wavelengths or spectral bands. In addition, it may be possible to gain additional information on details of the flare combustion--such as actual flame temperatures, the emissivity of the smoke, and burning times of the fuel particles.

Some of this work has been reported previously.[9]

EXPERIMENTAL BACKGROUND

For initial tests of the model, we have taken the magnesium/sodium nitrate/organic binder flare composition as an example, since this composition represents the most common military illuminating flare, and the one most thoroughly observed.

Various evidence indicates a temperature of about 1000 K at the burning surface: It has been observed,[7] using high speed photography, that most magnesium particles (m.p. 922 K) melt and ignite a few milliseconds before ejection from the solid, while some ignite a short distance away from the surface. Furthermore, decomposition of sodium nitrate, which produces the gas to blow the magnesium out of the flare, has been shown to take place very rapidly at 1000 K[10] at perhaps the same rate as in the surface of a burning flare. Finally, ignition temperatures of magnesium dust in air have been reported to be about 900 K.[11]

Plume temperatures have been determined by thermocouples[12] and by absolute brightness measurements[13] at the frequencies of the two maxima in the broadened sodium D line ($\sim$5800 and 6000 Å). Both types of measurements yield maximum temperatures in the vicinity of the computed adiabatic temperature, although they are uncertain by several hundred degrees. The position of the maximum temperature is found within a few inches of the surface in the thermocouple measurements cited.

Observations[14] indicate that the region of greatest brightness begins about one diameter from the surface. For stoichiometric mixes, the brightest region is fairly concentrated, whereas for fuel-rich mixes it is well spread out along the length of the plume.[3]

The shape of the flame and smoke plume depends on the orientation of the flare and on the surrounding air flow. For a flare burning upright in still air, the plume can be approximated as cone-shaped, with an apex angle of 15-30°. Plumes of large diameter (11 cm) flares may be luminous for a length of 1.5 to 2 meters to a point where the photometric brightness has decreased by a factor of about 10^6 from the maximum value.

Power spectra indicate that most of the luminous intensity is from the sodium D radiation,[1,2] a doublet of wavelength 589 nm. This radiation accounts for about 8% of the total heat of combustion in flares which have been optimized for efficiency of luminous output.

THE MODEL

Flow in the Plume

Combustion of a flare is quite complicated. In the body of the flare many reactions occur as the binder and oxidizer break down. Three phases are present near the surface as bubbles of gas push their way past remaining liquid and solid.

In the plume itself, the overall flow of material in three dimensions is complicated by strong local turbulence. A further complication of the flow is a detectably different movement of the gases and of the heavier particles.[15]

Equilibration of the reactants is slowed in many formulations by the high reaction temperatures of the metal particles.

Transfer of heat within and out of the plume occurs by a variety of radiation and conduction processes. The radiation is complicated in many flares by the light scattering of a highly reflective smoke.

The primary goal of this project was to predict radiative output rather than the details of combustion and flow. Therefore many simplifying assumptions were made regarding these latter phenomena.

First of all, the plume was modeled in one dimension with the flow of gases in one direction only--parallel to the plume axis. This most closely approximates the case of a flare burning upright, or else pointed downward in a forced downdraft.

The expansion of the plume perpendicular to the axis depends not only on the amount of air entrained but on viscous friction at the plume surface. Since this friction was not included in the model, the plume shape was arbitrarily specified as a cone, with apex behind the burning surface, as shown in Figure 1. Since the properties perpendicular to the axis were taken as constant the problem is still one-dimensional.

While the turbulence of the plume flow was not modeled, one of the major effects of turbulence--the entrainment of the surrounding environment (usually air)--was included. The model assumes continuous addition of air along the plume at an arbitrarily specified rate.

Conditions for the conservation of momentum in the plume are not imposed by the model. However an *ad hoc* calculation is made of the momentum change in the forward direction due to addition of environment (air).

We start with $mv = mF/A\rho_1$, where m is the mass of the cross-sectional slice of plume under consideration, F is the total mass flow across a cross-sectional plane, A is the cross-sectional area, and ρ, is the plume density. The change in plume density due only to the addition of the environment is given approximately by

$$\frac{d\rho_1}{dR} \approx \frac{\rho_1(\rho_2 - \rho_1)}{\rho_2(1 + R)},$$

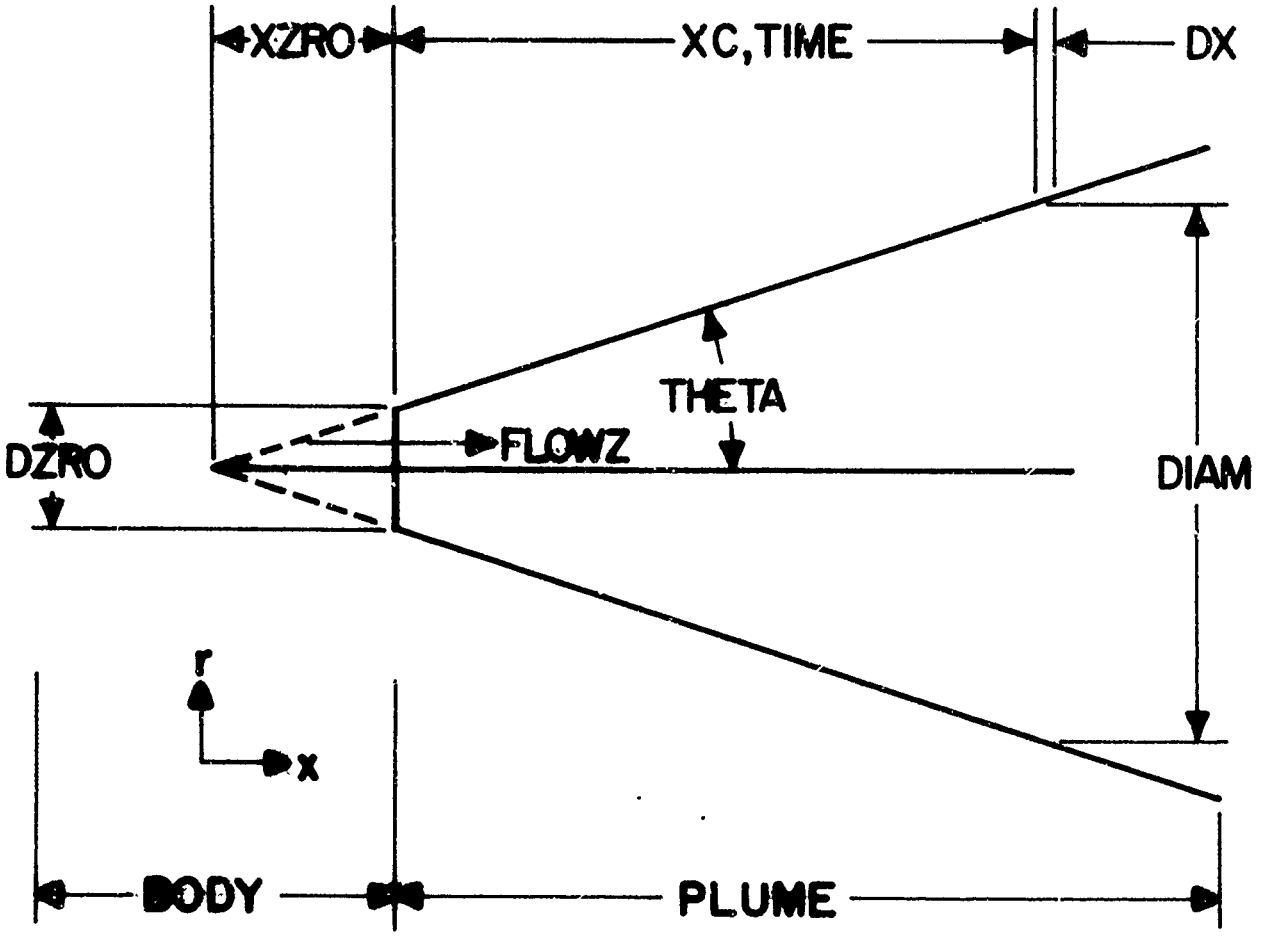

FIGURE 1. Plume parameters, labeled with the variable names used in the computer program. See Table A-1 in Appendix A.

where ρ_2 is the air density and R is the weight ratio of air to initial composition.

The change in A is computed from the assumed plume shape; and the change in the product mF equals the initial value, $m_o F_o$, times R. We then find:

$$\left.\frac{\partial mv}{\partial x}\right]_{mixing} \simeq \frac{m_o F_o (1 + R)}{A\rho}\left[\frac{\rho_2 + \rho_1}{\rho_2}\frac{dR}{dx} - (1 + R)\frac{d \ln A}{dx}\right] \quad (1)$$

where x is parallel to the plume axis.

If at any time the quantity in brackets is found to be positive a warning is printed out. When a cone-shaped plume is assumed it can be shown that the admission of air at a rate constant in distance will generally cause this quantity to be less than zero, as desired.

Temperature and Energy

A complete model of a flare flame in one dimension would satisfy the condition that the net energy flow into a point is zero (compare Eqn. 5.2 of Ref. 16):

$$\frac{d}{dx}\left(k\frac{dT}{dx}\right) - c_p v_x \rho \frac{dT}{dx} + Q(T) - R(T) = 0 \quad (2)$$

The first term represents heat transport in the direction of the flow by simple conductivity, radiation, and local turbulence. The second term represents net heat transport due to flow of material

containing a temperature gradient. The third term represents generation of heat by chemical reaction. The fourth term is loss of heat to the outside (perpendicular to the direction of flow) by radiation and simple conduction. Q and R are strongly dependent on temperature. In general, the thermal conductivity k, heat capacity c_p, velocity v_x, and density ρ have a much weaker temperature dependence.

With relatively minor simplifications, Eqn. (2) could reasonably be applied to the case of a flare plume, using the numerical techniques employed here. However, for a first effort, to save considerable programming and computer time, the first term in this equation (the thermal conductivity) was dropped. Since this term represents the thermal feedback, which aids greatly in driving the reaction, particularly in the early stages, it was necessary to arbitrarily specify Q rather than model it on physical principles, in order to get realistic results. This was done by arbitrarily specifying the rate at which the metal fuel enters the chemical reaction by vaporization, as will be explained in the section "Reactions in the Plume".

The loss of heat to the outside, represented by R(T), was broken into several parts to represent different types of radiation processes. The functional form of each was modeled to a first approximation. Non-radiative losses to the outside can be safely ignored. Thermal conductivity by molecular diffusion should be relatively small. Heat loss due to mixing in of air at the plume

surface is already taken into account by including this air with the reactants.

Equation (2) without the first term is solved numerically using a modification of the NASA computer program for complex equilibria.[17] The original program computes equilibrium compositions and temperatures from a given set of reactant materials and their enthalpies. Modifications were added to cause the program to automatically recompute equilibrium a specified number of times to represent closely spaced points along the plume. At each point, increments of air and of magnesium are added to the amount of initial reactants, to represent the continual mixing in of air and vaporization of magnesium. Radiation losses are computed based on temperature and emitter (sodium atom) concentrations at each point. These losses are subtracted from the enthalpy used in computing equilibrium at the next point. In this way, a temperature, composition, and radiation profile are constructed along the length of the plume. The radiant outputs are added up for all of the points, separately for each emission process, to obtain the total output of the amount of material considered.

The values of ρ computed thermodynamically at each point are used to recompute v_x, and thus variations of c_p, v_x, and ρ with changes in composition, temperature, and degree of reaction are automatically taken into account.

If it were desired to include thermal feedback, term number 1 of Eqn. (2), several iterations would need to be made at each distance increment in the

plume. The value of k which includes radiation, conduction, and turbulence contributions, would have to be specified, along with its temperature dependence, perhaps as one or two adjustable parameters.

Initial Conditions

The ideal starting point for the computations would be in the flare body at ambient temperature, well behind the burning surface. However, the illumination produced by the flare body is negligible, and probably its radiation at longer wavelengths can also be safely ignored because of its small size and low temperature compared to the plume. Therefore, to avoid the complications of modeling the processes taking place in the solid, particularly at the surface, and having to consider heat transfer to the surface, the computation is started in the gas phase at the burning surface. For the magnesium/sodium nitrate flare, a temperature of 1000 K is assumed. This is in reasonable agreement with the observations quoted earlier.

We must require that the change from ambient temperature to 1000 K occurs adiabatically. This is because of the neglect of the heat feedback (term number 1 of Eqn. (2)) and the assumption of no heat loss by the flare body. Just enough of the original fuel is assumed to have vaporized and entered the reaction to fulfill this adiabatic

condition. The remainder of the fuel has not yet entered the reaction. Under equilibrium conditions at 1000 K most oxidizers and binders are well decomposed.

Reactions in the Plume

Binder and oxidizer are assumed to have completely decomposed on leaving the flare surface. The magnesium is assumed to leave the surface in the form of the original particles, which gradually vaporize during flight.

Mixing and chemical equilibration among the decomposition products of binder and oxidizer, the magnesium vapor, and the entrained air is assumed to be instantaneous. This is in agreement with propellant models, where the thickness of the flame reaction zone above the burning surface has been calculated to be of the order of millimeters.[8]

The rate of reaction is then determined by the rate of vaporization of the magnesium and the rate of entrainment of air. An expression for the rate of vaporization of the magnesium particles as a function of local temperature and chemical environment (oxygen concentration) based on available particle burning models could be incorporated into the flare combustion model. But because of the mutual interaction between temperature and rate of burning, it would then be necessary to include the heat feedback term of Eqn. (2) in order to get the reaction started in a reasonable time. Since this term was omitted, the next best alternative was to specify a rate of vaporization of

magnesium. For want of better knowledge, we assumed that the magnesium vaporized at a constant rate in time until consumed. In fact, this is a crude compromise between the acceleration of the burning rate due to the increase in temperature when proceeding out into the plume and the decelerating effects of the decrease in particle size (surface area) and the accumulation of combustion products near the surface.

It should be pointed out, however, that due to neglect of heat feedback, the computed progress of the temperature of reaction will lag behind the real temperature for any degree of combustion.

An option was included in the computation to terminate vaporization of the magnesium before the particles are completely consumed. This option is useful for testing the hypothesis that certain fuels (e.g. aluminum) give lower output than expected due to incomplete combustion.

The magnesium particles were assumed to be at the local temperature or at the normal boiling point, whichever was lower. Appropriate corrections to the total enthalpy were made for the heat content of the unvaporized magnesium.

Radiation

As stated before, energy loss to the outside is taken to consist entirely of radiation. A number of kinds of radiation processes may be included, each with its own dependence on temperature and concentration of emitting species. Possibilities

include simple atomic line emission, atomic line emission in an optically dense medium, molecular band emission, and graybody radiation.

The computer program is presently set up with two radiation terms--sodium-D line emission in an optically dense medium and graybody radiation. Thus, the program can compute luminous intensity for any case where emission of a molecular species or of an atomic species other than sodium does not dissipate a significant (>2%) portion of the enthalpy. For somewhat greater accuracy, the emission of the sodium doublets at 568 nm and at 616 nm could have been included.

Sodium D Line Emission

In the usual case where the concentration of emitters is low enough such that reabsorption is negligible, the increase in intensity of a beam traveling from one side of the plume to the other is given by

$$\frac{dI}{dr} = \frac{hcN}{4\lambda\tau} \exp(-hc/\lambda kT),$$

where

h is Planck's constant
k is Boltzmann's constant
c is the velocity of light
λ is the wavelength

τ is the natural emission lifetime, and
N is the number of emitting atoms or molecules per unit volume.

The total emerging intensity is the integral of this expression across the plume; i.e. over r.

When N/τ is large, or the path is long, reabsorption must also be considered. Since absorption is dependent on the beam intensity and on the probability of absorption, both of which are frequency dependent, the intensity must be computed over small frequency intervals. Including absorption, we have (compare Eqn. 25, Ref. 18):

$$\frac{dI_\lambda}{dr} = -I_\lambda \frac{hc}{4\pi\lambda} B \frac{\lambda^2}{c} \frac{dN}{d\lambda} + \frac{hc}{4\lambda\tau} \frac{dN}{d\tau} \exp(-hc/\lambda kT) \quad (3)$$

where I_λ represents the intensity in unit wavelength interval centered at λ, $B = \lambda^3/2hc\tau$ is the Einstein transition probability per unit frequency for absorption, and $dN/d\lambda$ is the number density of emitting or absorbing atoms per unit wavelength. We rewrite this as

$$\frac{dI_\lambda}{dr} = -k_\lambda[I_\lambda - I_\lambda(eq)], \quad (4)$$

where

$$k_\lambda = \frac{\lambda^4}{8\pi c\tau} \frac{dN}{d\lambda}$$

is the absorption coefficient at wavelength λ, and $I_\lambda(eq)$ is the beam intensity at thermodynamic equilibrium in the wavelength interval λ to $\lambda + d\lambda$.

The total intensity I_λ emerging from the flare plume will be approximately the integral of Eqn. (4) across the plume (along r) provided that variations in temperature and emitter density along the plume length parallel to x are not too abrupt.

In a real flare the light path traverses regions with temperatures ranging from very high to ambient, which causes an absorption dip at the center of the spectrum of the line. For the purpose of including this feature in our calculation of the emerging Na D radiation we will make an exception to our basic assumption of uniform properties across the plume. We approximate the real situation by assuming that surrounding the plume, whose local diameter is l_1, is a thin sheath of thickness l_2, and zero temperature, and which has the same sodium atom concentration as within the plume. (Light emission at ambient temperature is negligible. The use of zero temperature is algebraically much simpler). Light reabsorbed here will be considered as *not* lost to the plume enthalpy.

Equation (4) then integrates to

$$I_\lambda = I_\lambda(eq)\ \exp(-k_{\lambda 2} l_2)(1 - \exp(-k_{\lambda 1} l_1)) \quad (5)$$

Subscripts 1 and 2 refer to the hot and cold paths, respectively.

To get the total intensity we must integrate Eqn. (5) over all wavelengths. To do this we need $dN/d\lambda$, in the expression for k_λ, i.e. we need to know the line shape.

Although the line shape is strongly influenced by both collision broadening and Doppler broadening, the effect of the latter becomes negligible in the wings of the line, which is where nearly all the radiation emerges for the high sodium atom densities typical of illuminating flares. We may then assume a Lorentzian line shape, so that

$$\frac{dN}{d\lambda} = \frac{N}{\pi} \frac{2/\Delta\lambda_L}{1 + [2(\lambda - \lambda_o)/\Delta\lambda_L]^2}$$

where $\Delta\lambda_L$ is the half-width at half height for the line as broadened by collisions, and λ_o is the wavelength at the line center.

On substituting this formula for $dN/d\lambda$ into k_λ and in turn into Eqn. (5), an expression was obtained which could not be integrated in closed or in series form. A numerical integration would have

been possible, but since $\Delta\lambda_L$, l_1 and l_2 vary at each point along the combustion path, the integration would have to be repeated many times, and would increase the costs of computation.

Since only the far wings of the line contribute significantly to the emerging light intensity we can make some approximations:

(1) Combining the above expressions for k_λ and $dN/d\lambda$ we obtain

$$k_\lambda = k_o/[1 + (2(\lambda - \lambda_o)/\Delta\lambda_L)]^2.$$

$k_o = \lambda^4 N/4\pi^2 c\tau\Delta\lambda_L$ is nearly constant over the line and equals the absorption coefficient at the center of the line when $\lambda = \lambda_o$.

For mathematical simplicity we use the same values of $\Delta\lambda_L$ and N (and hence of k_λ) in the hot and cold regions. This approximation is not serious in regard to $\Delta\lambda_L$ since it is only weakly dependent on temperature, because the line is pressure broadened. N varies much more drastically. On the other hand, the cold portion of the path must be relatively longer at lower temperatures. Therefore we will consider l_1 and l_2 as being effective lengths rather than actual distances.

Since we will use the values of $\Delta\lambda_L$ and N computed from the high temperature properties, the error will be in the estimation of the absorption dip. Since this dip is only about 20% of the total

intensity, errors in its calculation do not seriously affect the estimation of total output.

(2) It can be shown from Eqn. (5) that there is a maximum in I_λ as a function of k_λ, and that the wavelength λ_m at this point is given by

$$\lambda_m - \lambda_o = \pm \frac{\Delta\lambda_L}{2}\left(\frac{k_o l_1}{\ln(I_1/I_2 + 1)} - 1\right)^{\frac{1}{2}}$$

In evaluating the right side of this equation we can, to a good first approximation, set $\lambda = \lambda_o$ in the expression given earlier for k_o.

In the limit

$$k_o l_1 >> \frac{\lambda_m - \lambda_o}{\lambda - \lambda_o} \ln(I_1/I_2 + 1)$$

we have

$$K_\lambda \approx \left(\frac{\lambda - \lambda_o}{\lambda_m - \lambda_o}\right)^2 \left(\frac{\ln(I_1/I_2 + 1)}{I_1}\right).$$

The inequality expresses the condition that the optical thickness at line center should be much greater than 10, where unit optical thickness is defined as attenuation by the factor e. This should be true for most cases of practical interest.

We let $r = I_1/I_2$ and $y = (\lambda - \lambda_o)/(\lambda_m - \lambda_o)$. Substituting into the expression for k_λ and into Eqn. (5) and integrating over λ we obtain

$$I = I_\lambda(eq)(\lambda_m - \lambda_o)\int_{-\infty}^{\infty} (r + 1)^{-1/ry^2} \times[1 - (r + 1)^{-1/y^2}]dy \quad (6)$$

(3) Since the integral depends only on r, if we assume a constant ratio of hot path length to cold path length in the plume, we need perform the integration only once.

Since we assume that the line shape is dominated by collision broadening we evaluate the line width by:

$$\Delta\lambda_L = (2\lambda^2\sigma_L{}^2 N_T/\pi c)[2\pi RT(1/M_1 + 1/M_2)]^{\frac{1}{2}}$$

(compare Eqn. (104) of Ref. 18), where

$\sigma_L{}^2$ is the cross section for transition due to collisions,

N is the number density of all molecules,

M_1 is the atomic weight of the emitting atom or molecule

M_2 is the average molecular weight of the gases (in the plume)

Taking $\sigma_L{}^2 = 50 \times 10^{-16}$ cm^2 (Ref. 18 p. 171), $M_2 = 30$, $\tau = 10^{-8}$ sec, $\lambda = 5.89 \times 10^{-5}$ cm, N_T = Avogadro's number x PV/RT, and using the known

values of h, c, k, R, and M_1 we obtain

$$I_\lambda(eq)(\lambda_m - \lambda_o) = 111[\exp(-24416/T)][NPl_1/\sqrt{T}\ln(r + 1)]^{\frac{1}{2}}$$

in ergs sec^{-1} cm^{-3}. Thus the total intensity may be evaluated from Eqn. (6).

It is interesting to note that with the approximations used, the total emerging intensity is proportional to the square root of sodium atom concentration (N) and path length (l_1), rather than to the first power of these variables as in the optically thin case.

The simplifications made in deriving the radiative transfer equations of this section are based on the assumption of a high optical density--as stated earlier, an optical density much greater than 10 at line center. We may conveniently estimate these optical densities from the depth of the absorption dip in the spectrum of the broadened line. An examination of broadened sodium D spectra taken by Douda[19] over a variety of ambient pressures and sodium concentrations indicates that this treatment will not hold well enough for ambient pressures less than about 30 Torr at high sodium content or 150 Torr at a 5 percent $NaNO_3$ content.

Graybody Emission

As is well known, graybody radiation is

proportional to the area of emitting surface, the surface emissivity, and the fourth power of the temperature.

In a smoke, surface area may refer to either the total area of all the particles or the area of the periphery of the cloud, depending on whether the cloud is optically thin or thick, respectively. Computations indicate that typical magnesium oxide smoke clouds are highly reflective and therefore may be considered as optically thin.

Since we lacked sufficient information about particle sizes or the emissivity (and its temperature dependence) of the magnesium oxide produced we have expressed the time rate of graybody radiation loss per unit weight of original composition[20] by the simple product $\underline{a}T^4$, where $\underline{a}$ is a constant to be determined by trial, and is valid whenever magnesium oxide is the principal condensed phase produced.

A further calculation compares this radiation with the blackbody radiation which a flare plume of this size would emit (if the smoke were optically dense). The ratio is generally about 0.1. It can be thought of as the "emissivity" of the plume boundary.

The luminous intensity of the graybody radiation is computed and presented separately from the luminous intensity of the sodium D radiation.

An option is also included for computing the portion of the graybody radiation which is emitted into selected wavelength bands of the spectrum.

COMPARISON WITH EXPERIMENT

Before numerical calculations can be made, values must be assigned to various parameters which are included in the model, but which are not known *a priori* and were not derived theoretically. As presently set up, this includes the plume shape, the burning rate (surface recession), the proportion of admixed air, the vaporization rate of metal fuel, adjustment factors to the semi-theoretical expressions for the radiation processes, and the initial temperature.

In the following pages it is described how this was done using data from flares of the $Mg/NaNO_3$/binder composition. Comparisons are then presented of calculated and experimental results of this type of formula with a range of fuel/oxidizer ratios, environmental pressures, and environmental compositions, and with a small range of binder content. A comparison of predicted and experimental results for a selection of oxidizer compounds is also presented.

Adjustment of Parameters

The values of the adjustable parameters depend in a complex manner on the experimental observations which are to be satisfied. For instance, the graybody constant, the plume angle, and the rate of air mixing together determine the length of the visible part of the plume. The

particle vaporization rate, the plume angle, and the rate of air mixing are all important in determining the position of the brightest spot. The graybody and sodium D radiation constants, as well as the proportion of admixed air strongly affect the predicted luminous output.

Because of the strongly nonlinear effect of the model parameters on the computed results, no systematic procedure was found for adjusting the parameters to optimize the fit of predicted values to observed values. However, a large number of computations were performed using the formula 58% magnesium, 37.5% sodium nitrate, 4.5% epoxy binder and a 10.8 cm diameter, and a best set of parameters was selected.

The plume shape was assumed for simplicity to be conical. This is also in reasonable agreement with observations of flares burning upright. A plume angle of 0.6 radians was chosen. This is at the upper limit of observed values. The use of a narrower angle causes too long a visible plume with reasonable values of the sodium radiation constant and of the proportion of admixed air.

A burning rate of 0.25 cm/sec similar to that of the Mk 45 Aircraft Parachute Flare was assumed. The computed luminous output as a function of burning rate (only) passes through a broad maximum at a value of about 0.5 cm/sec, so that the results are moderately sensitive to decreases in burning rate but rather insensitive to assumed increases.

The initial temperature above the burning surface is assumed to be 1000 K. A small portion of the magnesium is assumed to have entered the reaction at this point so that a computation of the initial, adiabatic temperature yields this number. However, the results of luminous output are affected very little even by a value several hundred degrees either way. This is because so little luminous output occurs at the very short time the temperature remains at this low value.

The time required for complete vaporization of magnesium particles of size 400 μm was chosen as 0.1 seconds, a compromise between single particle burning experiments which indicate longer times[21] and observations of the position of maximum intensity[14], which indicate shorter times. In the case of finer particles a burning time proportional to the square of the initial diameter is to be assumed, in accord with both theory[22] and experiment.[21]

For the graybody radiation constant, a, the value 2.6×10^{-11} cal/(sec g deg^4) was chosen as giving a reasonable visible plume length with the plume angle chosen.

There is some experimental evidence[23] for emissivities as high as 0.5 for MgO and Al_2O_3 particles at high temperatures. This would result in nearly blackbody radiation intensity from the envelope of the smoke cloud.

From the value of a which was found to give the best results in the present calculations the graybody radiation efficiency of the smoke cloud

envelope is found to be much less than unity, perhaps about 0.1. This implies a much lower particle emissivity than in the experiments referred to.[23] In support of the present results, if the smoke were relatively black one might expect the atomic and molecular spectral features to be relatively swamped by a large graybody continuum, contrary to what is observed.[1,19]

The sodium D radiation was computed theoretically. Various approximations made in this calculation probably affect the absolute magnitude of the computed radiation more than they affect its dependence on temperature and sodium atom concentration. Therefore an adjustment factor was added for computing the absolute magnitude. The value of this factor is closely dependent on the value chosen for the graybody constant through the requirement mentioned earlier, that the sodium D radiation from a Mk 45 Aircraft Parachute Flare equal about 8% of the total heat of combustion. It is found that the value 2 satisfies this condition well enough for large (11 cm) flares. This is also reasonably close to the hoped-for value of unity which would have been obtained if the theoretical derivations could have been done exactly.

The model predicts greater outputs for smaller diameter flares than for large ones. This is contrary to experience, and may be caused by any of a number of the assumptions in the model, such as the assumption of complete combustion, the manner of computing admixed air, or the approximations in the radiative transfer model of the emerging

radiation. Here it has been dealt with by using a lower radiation constant for smaller flares--as small as 1.2 for a 3 cm diameter flare. Since there is no theoretical rationale for doing this, the model as it now stands should not be used to predict the result of varying flare diameter.

The ratio I_1/I_2 was more or less arbitrarily taken as 10. This value is reasonable in view of a computation of flame temperature based on the assumption that the intensity maximum equaled the equilibrium intensity at this wavelength.[13] Since the result was in the vicinity of the adiabatic temperature, I_1/I_2 must be much greater than unity. Fortunately, the model predictions turn out not to be critically sensitive to this parameter.

An attempt was made to determine this ratio from the broadened line spectrum in a systematic fashion, using the ratio of the apparent width at half height of the absorption dip at line center to the apparent width at half height of the entire line. However, it was realized that the continuum also had to be included and that this greatly complicated the computation. Therefore, this approach was abandoned.

One of the most difficult parameters to assign is the amount of admixed air. The computed results are fairly sensitive to this factor. As it is increased the optimum fuel/oxidizer ratio increases. For reasons given earlier the proportion of air was assumed to increase linearly with distance. The proportionality constant was taken such as to give a ratio of two parts air to one part original

composition by a distance 200 cm out in the plume. It is possible that a larger value, say 3, in combination with changes in the other parameters might give a better overall fit of the available data.

Partly on empirical and partly on theoretical grounds it was decided that this number should be proportional to the 2/3 power of pressure and inversely proportional to flare diameter for other than 10.8 cm flares burned at one atmosphere.

Computed and Experimental Values for Specific Cases

The temperature and flame brightness along the length of the plume were computed for a flare of composition 58% magnesium, 37.5% sodium nitrate, and 4.5% epoxy binder, and of diameter 10.8 cm, and the results are presented in Fig. 2. Since most of the parameters were adjusted by comparison with observations on this flare, the fit of computed to experimental results would be expected to be good.

Briefly, the length of the visible part of the plume (to a decrease of brightness by a factor of *ca.* 10^6) is seen to be about two meters. The sodium D output integrated over the entire plume length is 8.7% of the total combustion energy and the brightest spot is about 20 cm from the surface, all in accord with observation.

Trials with various proportions of admixed air, and with other parameters constant, are shown in Fig. 3a. The maximum in computed temperature, as well as the integrated sodium D output, seem to

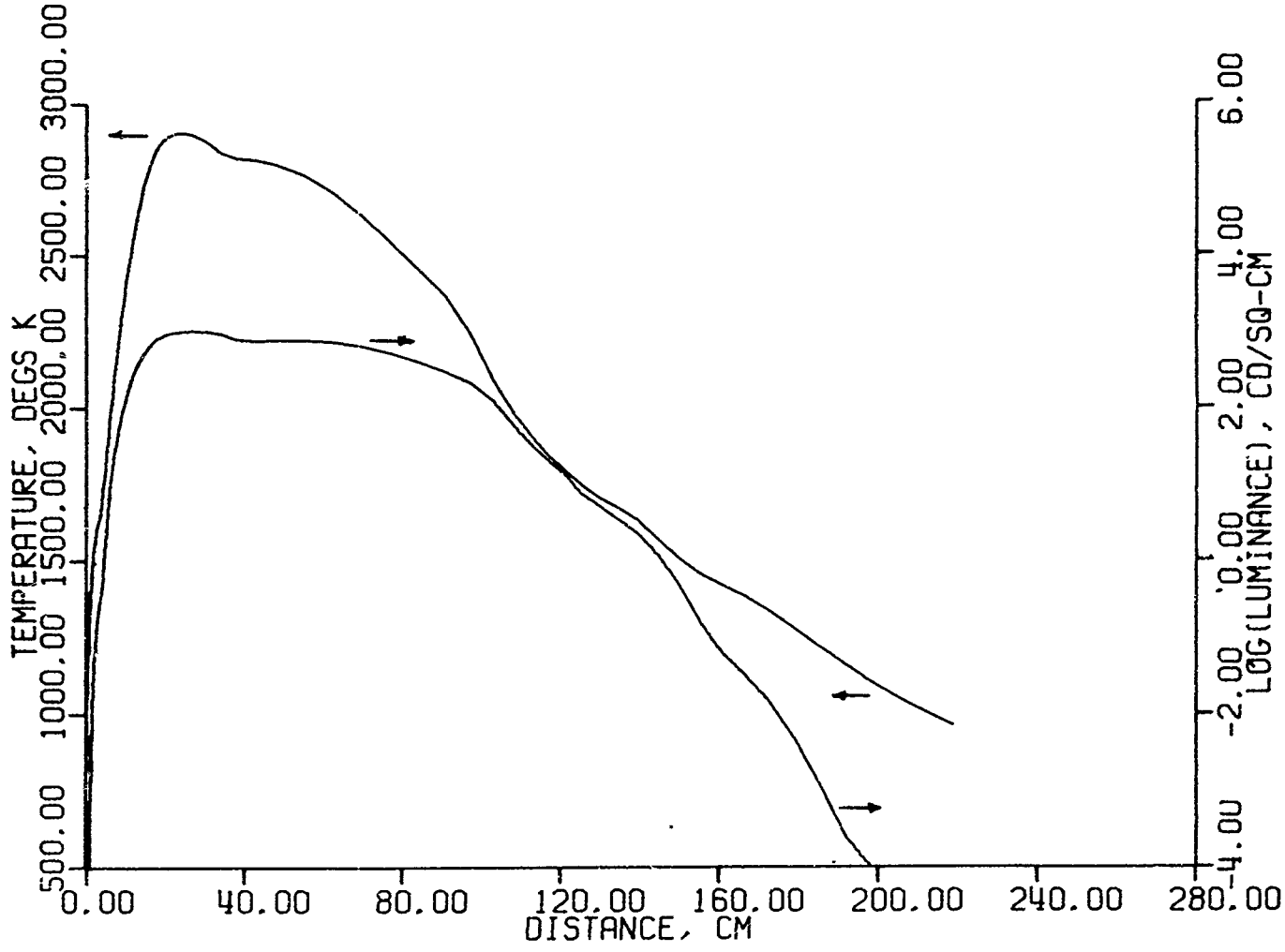

FIGURE 2. Computed flame temperature and flame brightness along the plume axis of a flare 10.8 cm diameter, 58% Mg, 37.5% $NaNO_3$, 4.5% epoxy binder. This is the plot from the run listed in Table A-3.

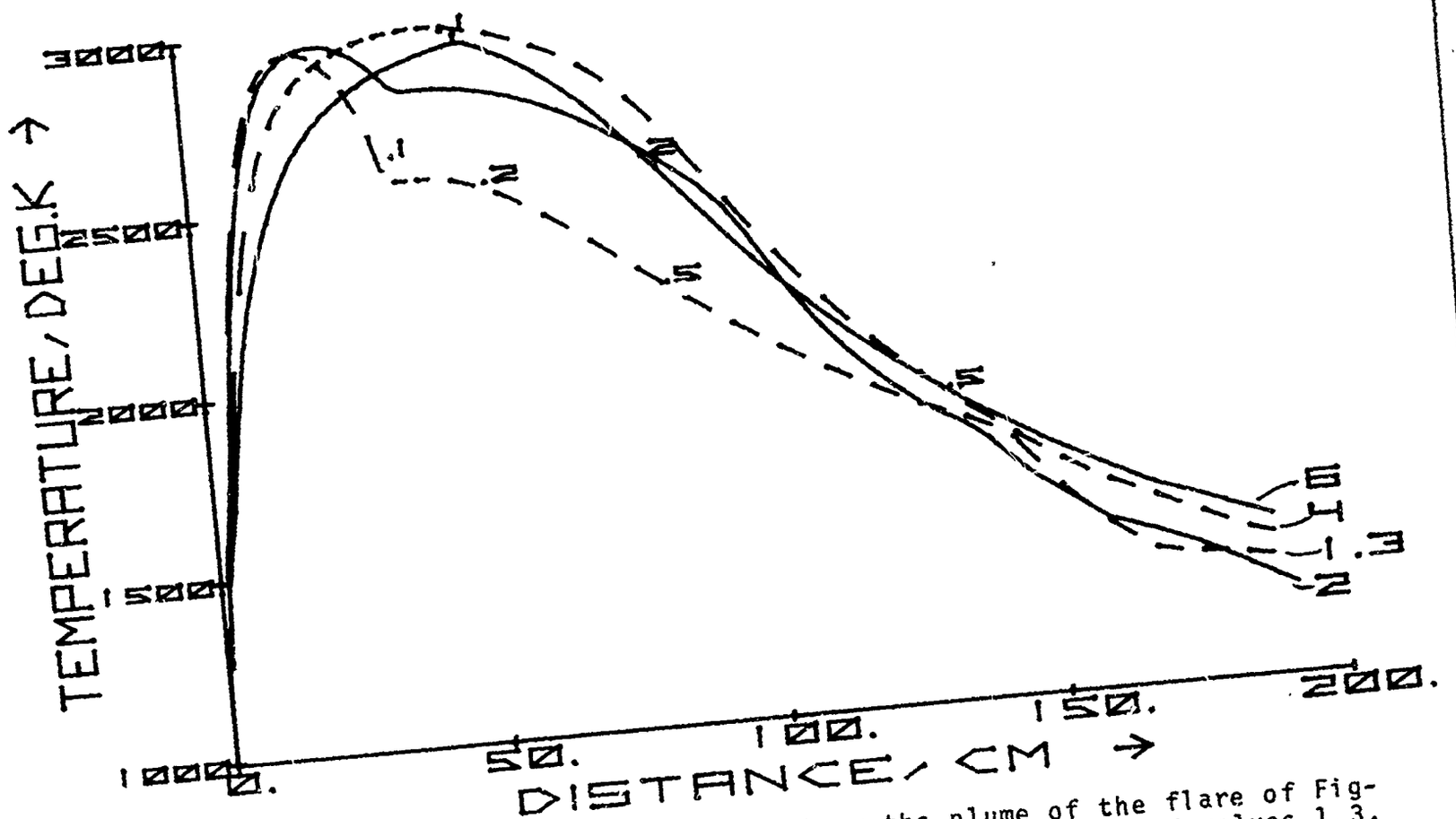

FIGURE 3a. Computed flame temperatures along the plume of the flare of Figure 2 but with air/composition weight ratios which have attained values 1.3, 2, 4, and 6 by a distance of 200 cm. Integrated luminous efficiencies are 22.8, 43.9, 46.9, and 30.2 kcd-sec/g, respectively. A few burning times are indicated as tenths of a second.

come at an air/composition weight ratio (200 cm) between 3 and 4. The value 2 gives nearly the maximum output, and as mentioned earlier other factors besides maximum output were considered in the selection of this ratio.

It is interesting to see what temperature could be expected for various proportions of air if no heat were lost from the system. For this purpose we have computed adiabatic flame temperatures as a function of degree of vaporization of magnesium and of proportion of air, for three different compositions of a $Mg/NaNO_3$/binder flare.[24] These temperatures are presented as topographic surfaces in Figs. 3b, c, and d. Composition paths representing the various proportions of air shown in Fig. 3a are superimposed on the appropriate adiabatic surface, Fig. 3c.

A comparison of experimental and calculated luminous efficiencies at various atmospheric pressures and for a number of fuel/oxidizer/binder ratios is presented in Table 1.

The agreement between prediction and experiment is fairly good, considering that the experimental values came from three different groups of workers. Generally it can be said that the calculation predicts a greater effect of pressure on fuel-rich mixtures, and a lesser effect of pressure on stoichiometric or oxidizer-rich mixtures than is found experimentally.

A comparison of experimental[26] and calculated luminous efficiencies in three atmospheric environments--air, nitrogen, and argon--is presented

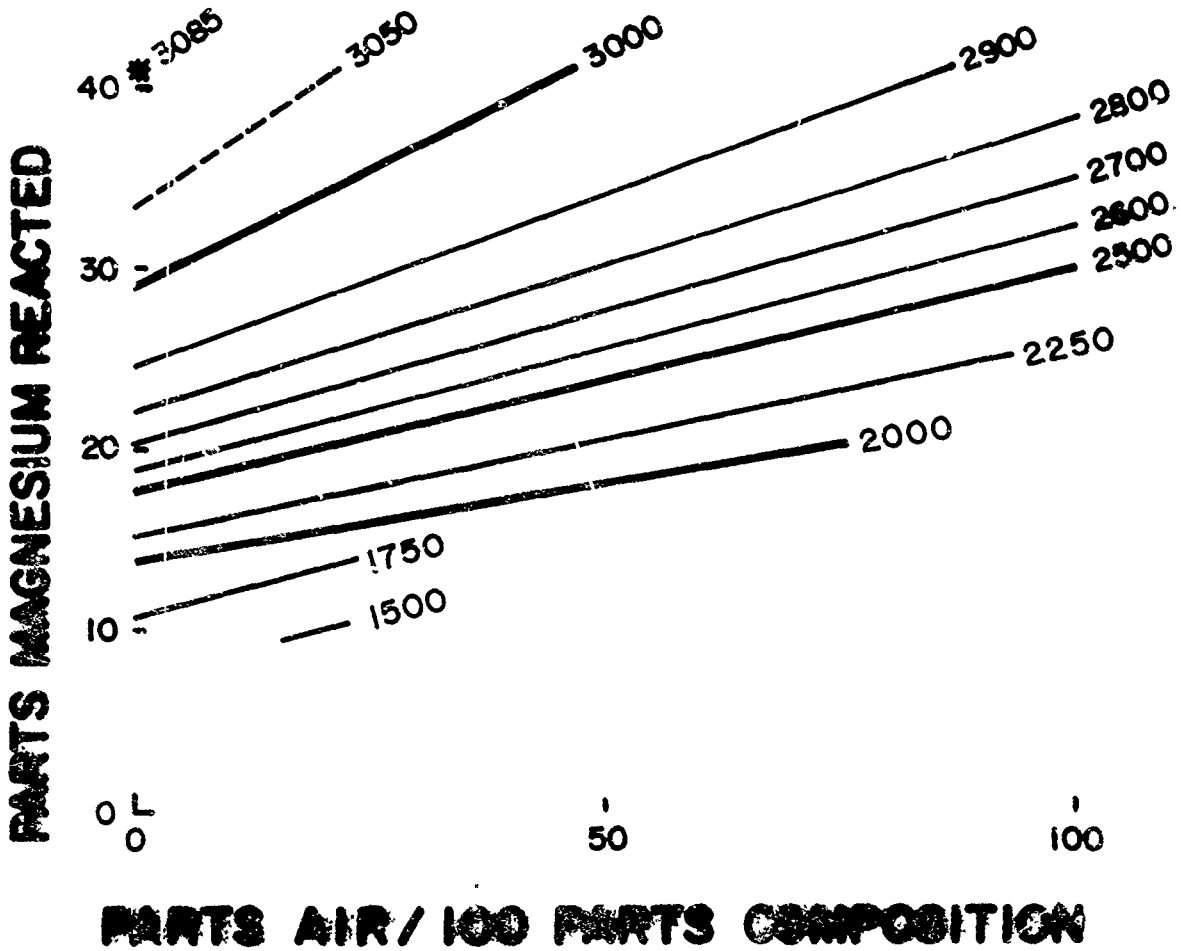

FIGURE 3b. Adiabatic flame temperatures at various degrees of reaction for a stoichiometric composition: 41% Mg/54.5% $NaNO_3$/ 4.5% binder. Contour lines are in degrees Kelvin. The asterisk indicates the maximum.

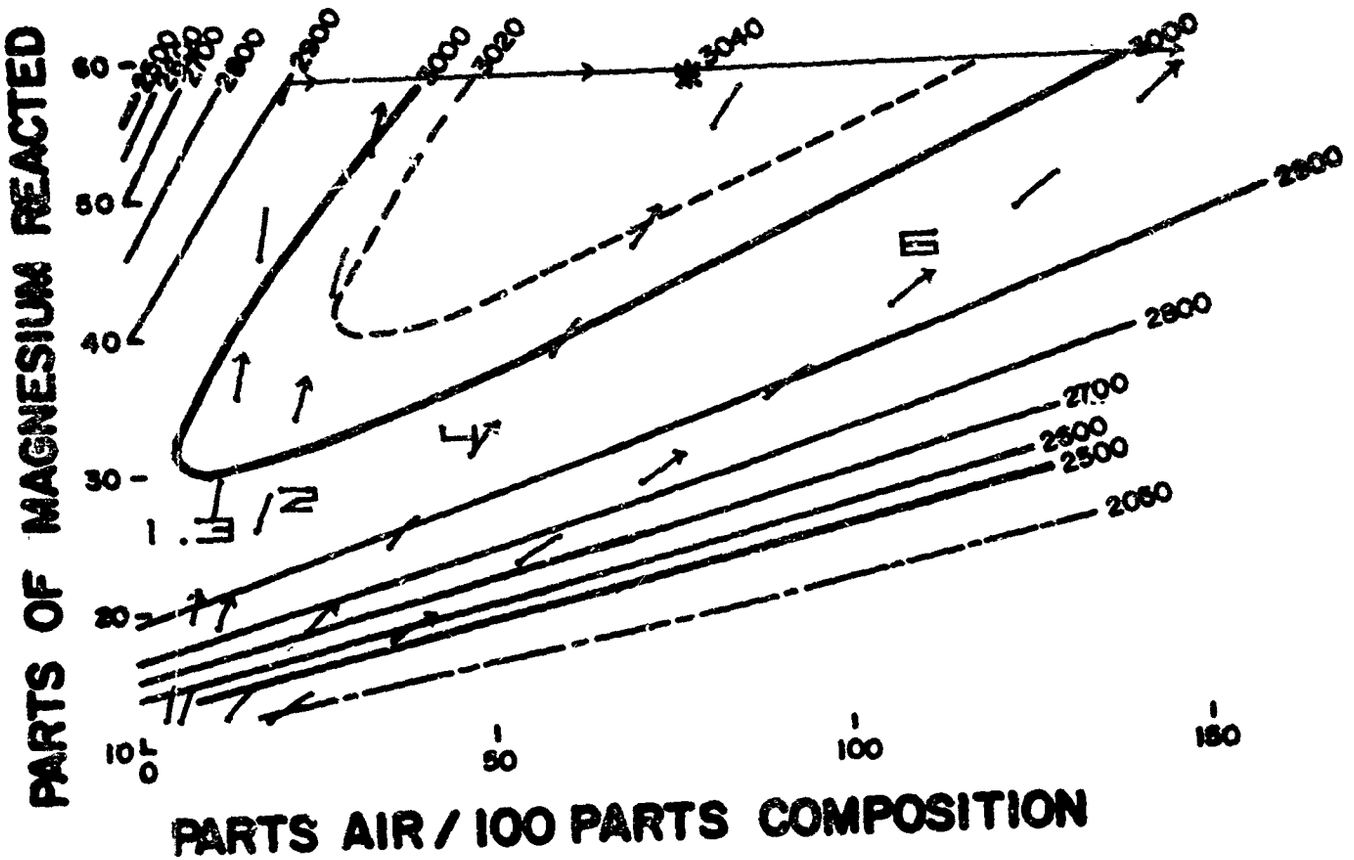

FIGURE 3c. Adiabatic temperatures for a standard, fuel-rich composition: 58% Mg, 37.5% $NaNO_3$, 4.5% binder. Arrows indicate combustion paths for the conditions of Figure 3a.

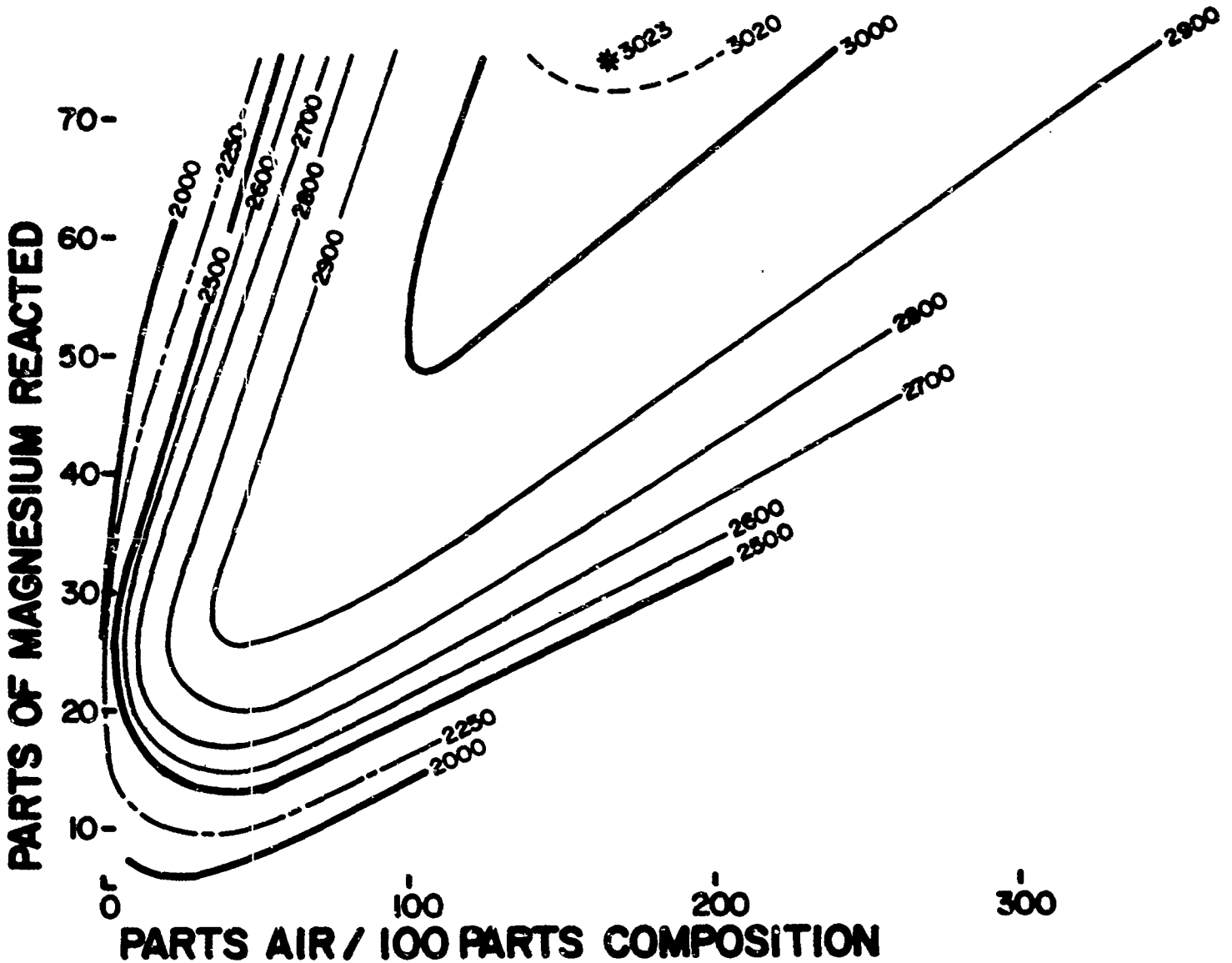

FIGURE 3d. Adiabatic temperatures for a very fuel-rich composition: 70% Mg, 25.5% $NaNO_3$, 4.5% binder.

TABLE 1. EFFECT OF AMBIENT PRESSURE. Comparison of predicted and observed luminous efficiencies, cd-sec/g, for magnesium/sodium nitrate/binder flares. From left to right the mixtures are increasingly fuel-rich.

Author	Resnick[25a]		Blunt[3]		Carrazza et. al.[25b]		Blunt[3]		Resnick[25a]	
Magnesium	31.8%		44.0%		60.0%		58.0%		59.1%	
Binder	9.1%		4.5%		0.0%		4.5%		9.1%	
Diameter	4.9 cm		3.4 cm		5.0 cm		3.4 cm		4.9 cm	
Pressure	Calc.	Obs.	Calc.	Obs.	Calc.	Obs.	Calc.	Obs.	Calc.	Obs.
1 atm	19 200	30 000	28 100	26 000	20 000	13 700	44 000†	44 000	35 500	35 500*
0.45 atm= 6 000 m**	17 300	13 400							25 100	25 000
0.2 atm= 12 000 m	15 200	9 500	23 700	24 000			20 000	33 000	17 500	19 700
0.0395 atm			14 400	11 000			5 400	11 400		
0.0295 atm= 24 000 m					12 700	230				

*Resnick presents luminous intensity and burning time, but not candle weight; therefore, this observation was arbitrarily equated to the predicted value and Resnick's other observations set relative to this one.

†The value of the sodium radiation constant for computations in this table was set so as to give agreement with this particular experiment.

**Equivalent altitude

in Table 2. The predicted values are seen to follow the experimental values semiquantitatively as fuel percent, binder content and the environment are changed.

The biggest disagreement is that computed values for a fuel-rich mixture in a nitrogen environment are much lower than the experimental ones. This is similar to the discrepancy for fuel-rich flares at low pressure (Table 1). Also, the computed superiority of argon over nitrogen is greater than that found experimentally.

The computed effect of going from 5% to 8% binder at the highest fuel percent is the reverse of that found in these experiments; however, general experience tends to confirm the computations that illumination efficiency decreases with increasing binder content when other factors are held constant.

Experiments and calculations to compare the effectiveness of various sodium-containing oxidizers are presented in Tables 3 and 4.

Table 3 compares calculated maximum temperatures and luminous efficiencies for magnesium-fueled formulas with a variety of sodium-containing oxidizers. The same grain diameter, burning rate, binder content, and magnesium/oxidizer equivalence ratio are assumed for all cases.

Of the five other oxidizers, only sodium superoxide is predicted to give greater luminous efficiency than sodium nitrate. The higher temperature predicted for the sodium perchlorate formulation is more than compensated for by the tieing-up of the atomic sodium as sodium chloride, which doesn't radiate well.

TABLE 2. COMPUTED AND EXPERIMENTAL[26] LUMINOUS EFFICIENCIES IN VARIOUS ENVIRONMENTS

Composition (wt. percent)		Relative Luminous Efficiencies (cd-sec/g:cd-sec/g)					
		Air		N_2		Ar	
Magnesium	Binder	Exper.	Calc.	Exper.	Calc.	Exper.	Calc.
40.0	5.0	0.57	0.43	0.27	0.25	0.36	0.44
47.5	5.0	0.85	0.74	0.17	0.13	0.27	0.25
55.0	5.0	1.00*	1.00*	0.10	0.048	0.14	0.10
40.0	8.0	0.68	0.57	0.20	0.14	0.23	0.27
47.5	8.0	1.00	0.84	0.077	0.053	0.10	0.11
55.0	8.0	1.07	0.97	0.032	0.015	0.032	0.035
60.0	8.0	1.03	0.95	0.013	0.0034	0.014	0.010

* Arbitrarily defined as unity. The absolute values calculated consistently with the computations in Table 1 are: Experimental, 63 500 cd-sec/g; computed, 54 000 cd-sec/g.

TABLE 3. PREDICTED LUMINOUS EFFICIENCIES, COMPARISON OF SODIUM-CONTAINING OXIDIZERS

Oxidizer	Percent Magnesium	Maximum Temp. (K)	Computed Luminous Efficiency (Kcd-sec/g)
$NaNO_3$	58.0	2960	43.5
$NaNO_2$	53.4	2855	39.0
$NaClO_4$	56.2	3057	37.0
NaO_2	58.7	2970	54.0
Na_2O_2	50.5	2525	26.5
$NaIO_3$	38.1	2852	16.6
25% $NaN_3/NaNO_3$	42.8	2736	32.0

The calculations assume a 10,8 cm grain diameter and a burning rate of 0.25 cm/sec. The formulas are all fuel-rich, and have the same magnesium/oxidizer equivalence ratio as the Mk 45 Aircraft Parachute Flare. 4.5% of epoxy binder is included in all cases.

TABLE 4. EXPERIMENTAL VERSUS COMPUTED LUMINOUS EFFICIENCIES FOR VARIOUS FORMULAS WITH A SODIUM-CONTAINING OXIDIZER

Oxidizer	Mg	Diameter (cm)	Experimental Efficiencies kcds/g	Experimental Efficiencies Relative	Calculated Efficiencies kcds/g	Calculated Efficiencies Relative	Experimental Reference
37.4% $NaNO_2$	58.1%	2.2		0.81	45.7	1.05	29
37.5% $NaNO_3$	58.0%	2.2		1.00	43.5	1.00	
39.5% $NaClO_4$	55.5%	3.3	32.0	0.52	31.8	0.68	3
38.0% $NaNO_3$	57.0%	3.3	62.0	1.00	46.5	1.00	
54.8% $NaClO_4$	40.2%	3.3	28.0	0.45	15.6	0.34	
51.2% $NaNO_3$	43.8%	3.3	39.0	0.63	24.2	0.52	
17.9% NaO_2 + 18.3% $NaNO_3$	56.8%	4.76	14.0	0.30	44.6 30.2*	1.09 0.74*	27
37.5% $NaNO_3$	58.0%	4.76	47.0	1.00	41.0	1.00	
57.0% $NaIO_3$	38.5%	3.3		0.36	18.5	0.39	28
37.5% $NaNO_3$	58.0	3.3		1.00	47.8	1.00	
25.0% NaN_3 + 38.6% $NaNO_3$	33.0	3.3		1.00	10.0	0.42	30
51.5% $NaNO_3$	44.0%	3.3		1.00	23.7	1.00	

See next page for footnotes.

Footnotes for Table 4.

*This calculation was done using the actual burn rate of 1.2 cm/sec. The other calculation for this formula, and that for the control used the actual burn rate of the control, 0.16 cm/sec. All other calculations used 0.25 cm/sec regardless of the experimental burning rate.

*The formulas are grouped in pairs each containing an oxidizer and a sodium nitrate "control" which was burned for comparison. The sodium nitrite flare is more fuel-rich, and the two sodium perchlorate flares are less fuel-rich than the corresponding sodium nitrate flares.

The sodium perchlorate flares contain 5% Laminac binder. The sodium azide flare contains 3.4% epoxy binder. The others contain 4.5% epoxy binder.

A comparison of predicted luminous efficiencies with experimental results for various sodium-containing oxidizers is given in Table 4. Each type of oxidizer is paired with the corresponding "control" formula using sodium nitrate. The calculations assume the same percentage compositions and grain diameters as had been used in the experiments. However, a common burning rate of 0.25 cm/sec was used except for the sodium superoxide calculations where the difference in the experimental burning rates between the odium superoxide formula and the sodium nitrate control was large enough to make a large difference in the calculations.

The model is fairly good in predicting the result of substituting sodium perchlorate or sodium iodate for sodium nitrate.

The difference between Tables 3 and 4 regarding the predictions for sodium nitrite are due to a difference in fuel/oxidizer ratio between the sodium nitrite and the sodium nitrate formulas in the case of Table 4. Nevertheless, the model fails to predict the moderate decrease for sodium nitrite actually observed. This may be the result of the basic model parameters selected, which tend to predict too high values for fuel-rich formulas and too low values for stoichiometric formulas.

The large decrease in output caused by substituting sodium superoxide for sodium nitrate is probably caused by the very high rate of burning which the superoxide flares had, and which cannot presently be predicted by the model. An excessive rate of burning probably causes numerous inefficiencies.

One of these is lack of time for radiation before the plume gets mixed with cold ambient air. This effect can be fitted into the model. The calculation employing the experimental burning rate predicts nearly half of observed decrease. The other effects may include incomplete combustion of the magnesium particles.

There is apparently also a failure in predicting a decrease in output with addition of sodium azide. The seriousness of the failure is uncertain since the experimental comparison was only a visual estimate.

DISCUSSION

Possible Improvements

The model predictions of luminous efficiency correlate moderately well with experimental results with $Mg/NaNO_3$ flares of a wide variety of fuel percent, a wide range of burning conditions, and performed by a number of investigators. The biggest discrepancies are probably due to the large fluctuations typical of flare performance. These are a reminder of the importance of many subtle factors, such as oxidizer particles sizes, loading pressures, cracks in the grain, etc., which would be difficult to model. There are even serious problems in getting agreement for a given set of flares observed with different experimental setups. The most that a simple thermodynamic model can do is predict the average of a large number of experiments.

Some of the systematic disagreements with experiment, such as the differences in the effect of decreased ambient pressure on compositions with different fuel/oxidizer ratios might perhaps be removed by reoptimizing the input parameters--plume angle, radiation constants, proportion of air, etc.

While doing this, a few refinements might be useful. For instance the graybody constant might be made proportional to the weight percent of condensed phase present in the reacting mixture. The rate of air mixing might be made proportional to the percent of volatile material (binder and

oxidizer) in the original composition, or even to the reciprocal of the instantaneous density, on the grounds that it is the rush of gas that entrains the environment.

There are several major refinements which would be satisfying from a theoretical viewpoint, and which might also bring better agreement with experiment. First, the inclusion of radiative feedback would enable at least an estimation of burning rates. A consideration of feedback is also necessary to the inclusion of a particle burning model, where the rate of vaporization of the metal particles would be expressed as a function of local temperature and oxygen content.

A consideration of the effect of local oxygen content on particle burning would probably improve predictions of performance of fuel-rich compositions in oxygen-poor environments.

Applications and Limitations

The model as set up is somewhat open ended. There is no sharp line between formulations and conditions which can be computed and those which cannot. At the one extreme are systems which can be computed quantitatively and reliably simply by furnishing input data as derived in this report on punch cards to the computer program as presented in the Appendix. At the other extreme are systems for which the computer program presented here would be a useful starting point, but would require major revisions.

In between are cases where after minor additions or deletions of statements to the program, and/or the examination of experimental data to obtain certain input data, quantitatively or qualitatively reliable results could be computed.

Thus, simply by supplying the standard NASA reactant cards[17] one may estimate sodium D radiation in absolute units for any formulation where MgO (or a condensed phase of similar emissivity) accounts for most of the radiative output. For instance, formulations of the type Mg/binder/X, where X is a sodium-containing oxidizer may be compared. This may be done for any desired ambient pressure or percent composition.

With the same ease one may compare sodium D radiation among formulations, all of which have a common graybody emitter of properties different from MgO. For instance, the above comparison could be made using aluminum instead of magnesium as fuel. The absolute values of the results would not be reliable, however, unless one comparsion with experiment using aluminum fuel were made.

Comparative estimates of other radiative processes besides sodium D emission may also be made by inserting the appropriate emission formula at the place in the program where radiation is calculated. For the case of atomic line emission or emission from an electronically excited state of a polyatomic species of relatively narrow band width the rate of emission would be proportional to

$$[X]e^{-h\nu/kT},$$

where [X] is the concentration of the emitting species as computed by the thermodynamic calculation, and $h\nu$ is the energy of the upper level. For instance, a comparison of the emission from the $^2\pi$ state of BaCl at 5200 ± 100 Å for the formulas $Mg/Ba(NO_3)_2/C_6Cl_6$ versus $Mg/Ba(ClO_4)_2$ may be possible in this way.

The expression used for sodium D radiation could readily be adapted to other lines broadened by passage through a region of high optical density.

More difficult is the estimation of radiation in absolute units, as would be necessary for a comparison of two different lines in the same formula. This requires that an adjustment factor, which represents the radiative lifetime of the excited state and compensates for other approximations, be added to the expression given above. This is most easily done by calibration against power spectra already available. For instance, to compare Na-D against $^2\pi$ BaCl radiation in a formula including Na, Ba, and Cl, it is first necessary to "calibrate" the computation of the BaCl emission (calibration of Na-D has already been done) by means of an available power spectrum for a formula which also contains Ba and Cl (but not necessarily Na).

Of still greater difficulty is the computation of emission from electronic states where the band spread is not small compared to the center frequency. Not much consideration has been given in this project to a derivation of the appropriate radiation formulas.

Of greatest difficulty would be the computation of lines which overlap in a spectral region of high optical density. Derivation of the appropriate radiation formulas and their insertion into the program would probably require a major new effort.

CONCLUSIONS AND RECOMMENDATIONS

The model of flare plume combustion and radiation as presented here has been shown to give predictions of luminous output which are in qualitative or semiquantitative agreement with experiments on magnesium flares of a wide range of compositions, and burning under a wide range of environmental compositions and pressures.

It should be useful for predicting radiant or luminous output with new formulas, and for optimizing the ratios of the various components in the proposed formulas because it makes use of all of the thermodynamic information of the components in a systematic fashion. The method used herefore has been to compute single thermodynamic parameters, such as heat of combustion, the adiabatic flame temperature, and the emitter concentrations and to use these as a qualitative guide in estimating output.

It is recommended that theoretical and experimental input parameters be obtained from the literature such that the model can be used for predictions of output of colored flares and of infrared decoy flares.

It is also recommended that the model be refined by (1) reoptimizing the arbitrary input parameters (2) including a heat feedback term in the basic equation and (3) including the dependence of the rate of fuel combustion on temperature and oxygen concentration.

REFERENCES

1. B. E. Douda, R. M. Blunt and E. J. Bair, J. Opt. Soc. Am. 60, 1116-1119 (1970).

2. B. E. Douda and E. J. Bair, J. Opt. Soc. Am. 60, 1257-1261 (1970).

3. R. M. Blunt, *Spectral Distribution of Different Regions of Illuminating Flare Flames*, RDTR No. 220, Naval Ammunition Depot, Crane, Indiana (December 1972). Available NTIS-AD No. 757663.* See also the references contained therein. The author does not give values for luminous intensity, but his raw data permit an estimate of these values.

4. D. R. Dillehay, *Possible Mechanisms for Burning Rate/Candlepower Enhancement in Illuminants* in *Proceedings--Third International Pyrotechnics Seminar* held at Colorado Springs, Colorado, 21-25 August 1972. (Sponsored by Denver Research Institute, University of Denver), p. 1. Available DDC-AD No. 913408L.**

---

* Available NTIS indicates that this document is available from National Technical Information Service, 5285 Port Royal Road, Springfield, Virginia 22161.

** Available DDC indicates that this document is available from Defense Documentation Center, Cameron Station, Alexandria, Virginia, 22314.

5. R. L. Tischer, *Effect of Entrained Air in Determining Optimum Flare Compositions* in *Proceedings--Second International Pyrotechnics Seminar* held at Snowmass-at-Aspen, Colorado, 20-24 July 1970. (Sponsored by Denver Research Institute, University of Denver), p. 425. Available DDC-AD No. 913407L.

6a. *Exploratory Development of Illuminating Flares*, AFATL-TR-68-91, Air Force Armament Laboratory, Eglin AFB, Florida (August 1968). Available NTIS-AD No. 848086.

6b. *Exploratory Development of Illuminating Flares--Phase II* AFATL-TR-69-107, Air Force Armament Laboratory, Eglin AFB, Florida (August 1969). Available NTIS-AD No. 872686.

7. J. L. Eisel and D. E. Zurn, *Physicochemical Details at the Surface of Burning Illumination Flares*, NWC-TP-5726, Naval Weapons Center, China Lake, California (April 1975). Available NTIS-AD No. A009356.

8. See e.g. M. W. Beckstead, R. L. Derr, and C. F. Price, *A Model of Composite Solid-Propellant Combustion Based on Multiple Flames*, AIAA Journal 8, 2200 (1970).

9. J. E. Tanner, *A Mathematical Model of Flare Plume Combustion and Radiation*, in *Proceedings--Fourth International Pyrotechnics Seminar*, held at Steamboat Springs, Colorado, 22-26 July 1974. (Sponsored by Denver Research Institute, University of Denver).

10. J. W. Mellor, *A Comprehensive Treatise of Inorganic and Theoretical Chemistry* (John Wiley and Sons, Inc., New York, N. Y., 1961), Supplement II, Vol. II, p. 1243.

11. H. Ellern, *Military and Civilian Pyrotechnics* (Chemical Publishing Co., Inc., New York, 1968), p. 296.

12. J. T. Hamrick and L. C. Rose, *Temperature Distribution in the Plume* in *Exploratory Development of Illuminating Flares--Phase II*, AFATL-TR-69-107, Air Force Armament Laboratory, Eglin AFB, Florida (August 1969), p. 50-64. Available NTIS-AD No. 872686.

13. P. L. Blackshear, et. al., *Flare Characteristics and Spectral Analysis* in *Exploratory Development of Illuminating Flares*, AFATL-TR-68-91, Air Force Armament Laboratory, Eglin Air Force Base, Florida (August 1968). Available NTIS-AD No. 848086.

14. H. R. Waite and R. R. Weaver, *Luminous Intensity Distribution* in *Exploratory Development of Illuminating Flares--Phase II*, AFATL-TR-69-107, Air Force Armament Laboratory, Eglin Air Force Base, Florida (August 1969), p. 98. Available NTIS-AD No. 872686.

15. P. L. Blackshear and J. Alexander, *Flame Characteristics and Particle Study* in *Exploratory Development of Illuminating Flares--Phase II*, AFATL-TR-69-107, Air Force Armament Laboratory, Eglin Air Force Base, Florida (August 1969), p. 65. Available NTIS-AD No. 872686.

16. A. G. Gaydon and H. G. Wolfhard, *Flames, Their Structure, Radiation, and Temperature*, (Chapman and Hall Ltd., 1970), Third Edition.

17. S. Gordon and B. J. McBride, *Computer Program for Calculation of Complex Chemical Equilibrium Compositions, Rocket Performance, Incident and Reflected Shocks, and Chapman-Jouguet Detonations*, NASA SP-273, Lewis Research Center (1971). Available NTIS-N71-37775.

18. A. Mitchell and M. W. Zemansky, *Resonance Radiation and Excited Atoms* (Cambridge University Press, New York, N. Y., 1971). See especially equations 25, 92 and 104.

19. B. E. Douda, *Radiative Transfer Model of a Pyrotechnic Flame*, RDTR No. 258, Naval Ammunition Depot, Crane, Indiana (September 1973), available DDC-AD No. 769737 and J. Quant. Spectrosc. Radiat. Transfer 14, 1091 (1974).

20. In the previous work (Ref 9) the formula aT^4 was inadvertantly taken as being the rate of graybody radiation *per gram of oxidizer* contained in the original composition. This is in principle erroneous since the amount of solids emitting graybody radiation should be proportional to the amount of fuel, not oxidizer. As a result, it has been necessary to recalculate or delete all of the figures and tables presented there, except those for a composition 58% magnesium and 4.5% binder. The qualitative conclusions reached earlier are still correct, however.

21a. H. M. Cassell and I. Liebman, *Combustion and Flame* 6, 153 (1962).

21b. R. P. Wilson and F. A. Williams, *Thirteenth Symposium (International) on Combustion* (The Combustion Institute, Pittsburg, Pa., 1971), p. 833.

21c. J. R. Richard, R. Delbourgo and P. Laffitte, *Twelfth Symposium (International) on Combustion* (The Combustion Institute, Pittsburg, Pa., 1969), p. 39.

22. H. Wise, J. Lorell, and B. J. Wood, *Fifth Symposium (International) on Combustion* (The Combustion Institute, Pittsburg, Pa., 1955) p. 132.

23. D. J. Carlson, *Emittance of Condensed Oxides in Solid Propellant Combustion Product* in *Tenth Symposium (International) on Combustion* (The Combustion Institute, Pittsburg, Pa., 1965), p. 1413.

24. A similar set of computations was performed by R. L. Tischer (Ref. 5). However his computations are for complete combustion of the fuel present in the formula.

25a. S. Resnick, *Simulated High Altitude Tests of Illuminating Compositions*, TR No. 2166, Samuel Feltman Ammunition Labs., Picatinny Arsenal, Dover, N. J. (April 1955). Available DDC-AD No. A61693.

25b. J. A. Carrazza, Jr., B. Jackson, Jr. and S. M. Kaye, *New Flare Formulations for High Altitude Application*, TR No. 3360, Picatinny Arsenal, Dover, N. J. (October 1966). Available NTIS-AD No. 641957.

26. D. R. Dillehay, *Illuminant Performance in Inert Atmospheres*, in *Proceedings--Fourth International Pyrotechnics Seminar* held at Steamboat Springs, Colorado, 22-26 July 1974, (Sponsored by Denver Research Institute, University of Denver).

27. C. E. Dinerman and J. E. Tanner, Jr., *An Investigation of Sodium Superoxide as an Oxidizer in Magnesium-Sodium Nitrate Illuminating Flare Compositions*, RDTR No. 291, Naval Ammunition Depot, Crane, Indiana (February 1975). Available DDC-AD No. B002 867L.

28. H. A. Webster III and C. W. Gilliam, *Spectral Characteristics of Flares Containing Sodium Iodate* in *Proceedings of the Fourth International Pyrotechnic Seminar*, 22-26 July 1974 at Steamboat Springs, Colorado (Sponsored by Denver Research Institute, University of Denver) and RDTR No. 276, Naval Ammunition Depot, Crane, Indiana (June 1974), available DDC-AD No. 782510.

29. Unpublished results of C. E. Dinerman (Naval Ammunition Depot, Crane, Indiana).

30. C. E. Dinerman, *An Attempt to Increase the Luminous Output of Magnesium-Sodium Nitrate Flares by the Introduction of Nitrogen-Containing Compounds*, RDTR No. 278, Naval Ammunition Depot, Crane, Indiana (June 1974), available DDC-AD No. 921142L and H. A. Webster III, *Visible Chemiluminescent Flare* in *Pyrotechnic Exploratory Development and Pollution Abatement Semi-Annual Report*, RDTR No. 250, Naval Ammunition Depot, Crane, Indiana (August 1973), available DDC-AD No. 912250L. Quantitative data are not presented, but light output of the two formulations is stated to be essentially the same.

APPENDIX A
THE COMPUTER PROGRAM

The basic computer program is that of Gordon and McBride* for computation of chemical equilibrium. The unneeded subroutines ROCKET, RKTOUT, FROZEN, SHCK and DETON were deleted. A new subroutine, INCRMT, was added to add increments of the surrounding atmosphere and of magnesium vapor to the reaction mixture corresponding to increments of time and distance from the burning surface, and to compute radiation losses.

A few statements were added to subroutine SEARCH to determine the species number of the particulate fuel.

Subroutine THERMP was modified to allow information on the assumed conditions of combustion and a specification of desired output to be read in.

An entry point in subroutine EQLBRM was arranged so that computations would loop around through INCRMT and EQLBRM until the computed flame temperature had dropped to a suitable value (now set at 1000 K) or until a limited number of points had been computed.

The flow charts of these changes are shown in Figs. A-1 to A-3. A printout of the modified portions of the NASA program is given in Table A-1. A list

---

*S. Gordon and B. J. McBride, *Computer Program for Calculation of Complex Chemical Equilibrium Compositions, Rocket Performance, Incident and Reflected Shocks, and Chapman-Jouguet Detonations*, NASA SP-273, Lewis Research Center (1971). N71-37775, AD 727607.

TABLE A-1.

IMPORTANT VARIABLES ADDED TO THE NASA PROGRAM

Name (dimensions)	Description
BD(5)	Graybody energy radiated since the last point in the wavelength band designated by the corresponding BL, calories/R/gram of initial mixture.
BL(5,2)	Wavelength (μm) limits of graybody radiation band desired.
BL1(5)	BL(I,1).
BL2(5)	BL(I,2).
BRT	Rate of recession of flare surface, cm/sec.
BRIT	Flame brightness in the vicinity of the point computed, candela/cm^2.
BUF(63)	Buffer used by the plot subroutine.
CBB	Adjustable graybody radiation constant in calories/R/deg^4/sec/gram of initial mixture.
CNAD	Adjustable sodium-D radiation constant, dimensionless.
CON	The right side of Eq. (1).
CONC(10)	g-moles of j-th species/g of mixture including admixed environment, and excluding unvaporized fuel.
DEN	Density of flare composition, g/cm^3.
DTL	Sought-for temperature change between points.
DX	Current distance between points.

TABLE A-1 (cont.)

DZRO	Diameter of flare, cm.
EFF	Computed graybody emission relative to the blackbody radiation from a plume of the same diameter.
EMARAY(202)	Values of flame brightness stored for plot.
FLOWZ	Flow of material across the plane of the flare surface, g/sec.
HSUBO	Enthalpy of reacting mixture, including environment, excluding unvaporized fuel cal/R/g, as in original NASA program.
KB	Number of radiation bands desired.
KSP	Number of species concentrations to be printed out.
KRON	This variable equated to zero to compute adiabatic temperatures. Otherwise, equated to unity.
L12	l_1/l_2, the effective ratio of hot path length to cold path length for the emerging radiation.
NA	Species number of atomic sodium.
NCF	Condensed species number of the fuel.
NEND	Maximum number of points desired.
NMG	Species number of the fuel.
NPLPTS(202)	Number of points to be plotted.
NX	Current point number.
PLOTT	Logical variable. "True" if a plot is desired.

TABLE A-1 (cont.)

PLT	Suppresses plotting of the first point.
POWR	The amount of admixed air is proportional to the distance to a power. Has generally been equated to unity.
RAD1	The integral in Eq. (6).
RBB(5)	Graybody radiation for current point, cal/R/g of original composition.
RHO(5)	Mixture density including unvaporized fuel, g/cm^3.
RNAD(5)	Sodium-D radiation for current point, cal/R/g of original composition.
SBD(5)	Total graybody radiation in a given wavelength band, units of calories/g for final printout.
SBL	Total luminous output due to graybody radiation, cd sec/g.
SPC(9,2)	Names of species whose concentrations are desired in the printout.
SRBB(5)	Total graybody radiation, units of cal/g in final printout.
SRNAD(5)	Total sodium-D radiation, units of cal/g in final printout
SRNADL	Total luminous output due to sodium-D line, cd sec/g.
STLUM	Total luminous output, cd sec/g.
T(5)	Current temperature.
T2ARAY(202)	Stored values of temperature for plot.
THETA	Assumed half-apex-angle of plume, radians.

TABLE A-1 (cont.)

TI	Guess of initial temperature, K.
TIME(5)	Current time of flight, sec.
TLUM	Luminous output at current point, cd sec/g.
TWF	Assumed time for complete vaporization of fuel, sec.
WF	Final weight percentage of vaporized fuel, usually equal to the percentage specified on the corresponding "reactants" card.
WFA	Weight ratio of admixed environment to composition by 200 cm from the surface, x 100.
WI	Initial weight percentage of vaporized fuel.
WT(14)	Weight percentages of reactants.
XC	Current distance from the flare surface.
XCARAY(202)	Stored values of XC.

FIGURE A-1. Modifications to Subroutine EQLBRM

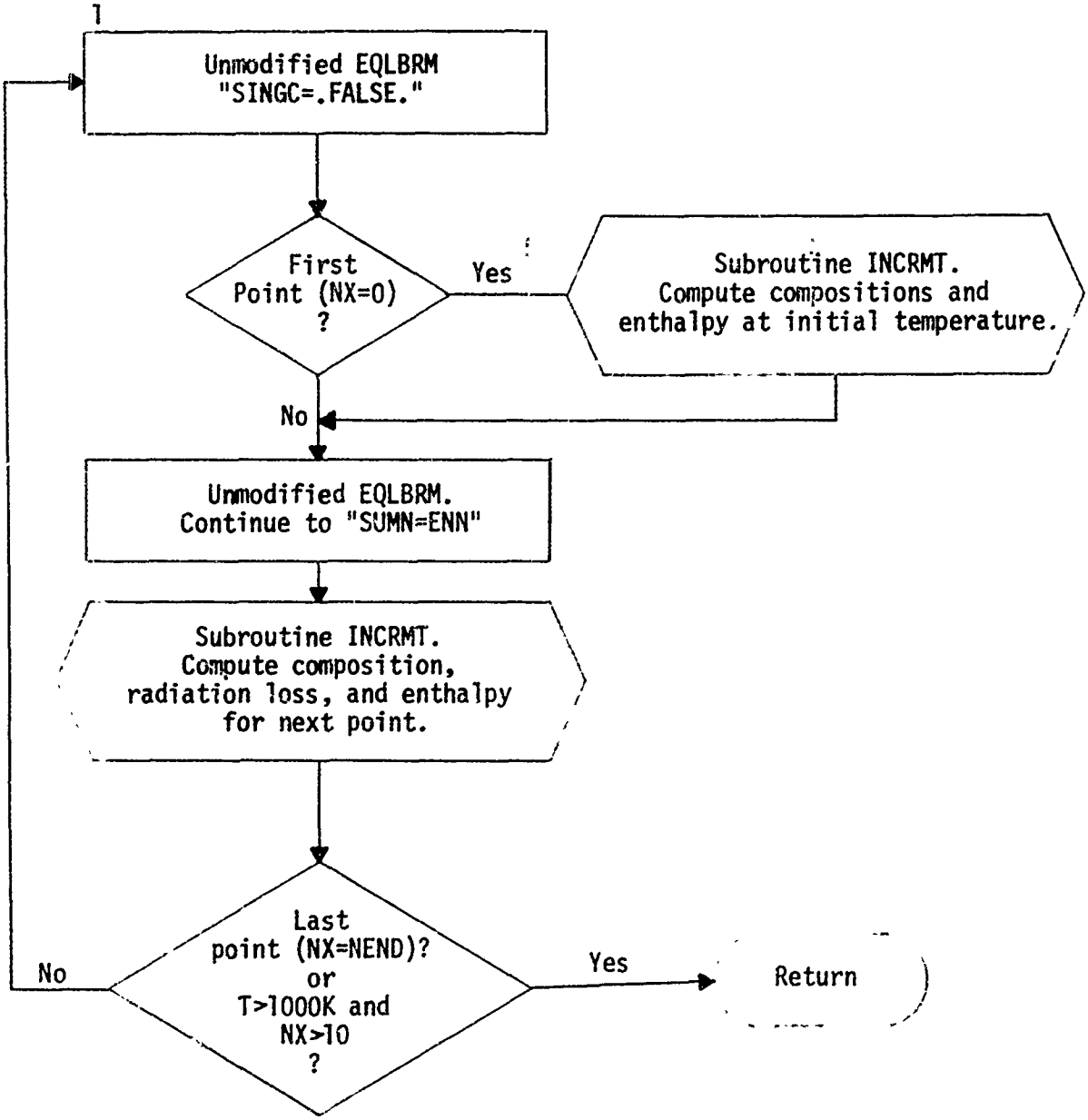

FIGURE A-2. Modifications to Subroutine THERMP

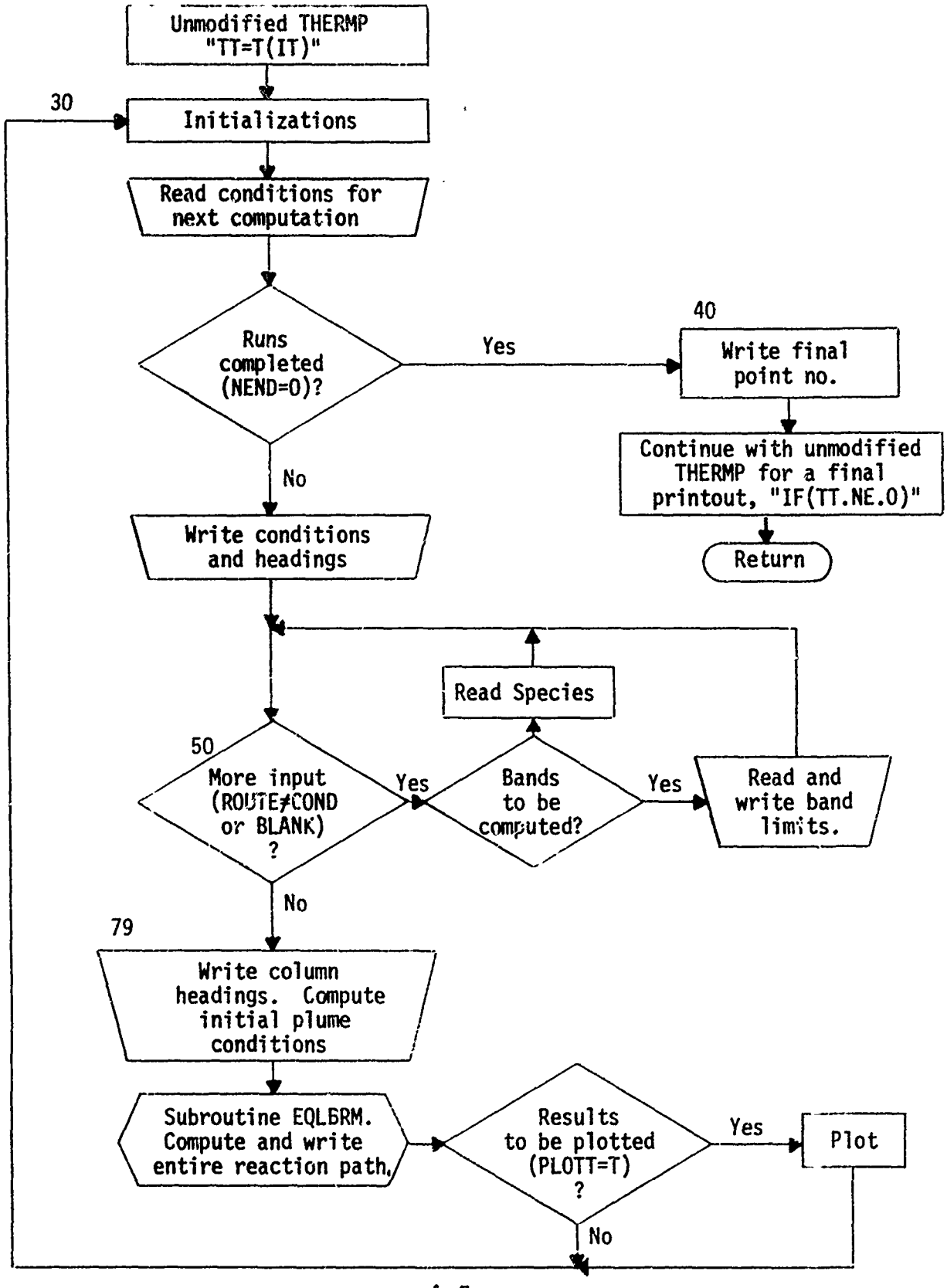

FIGURE A-3. Subroutine INCRMT

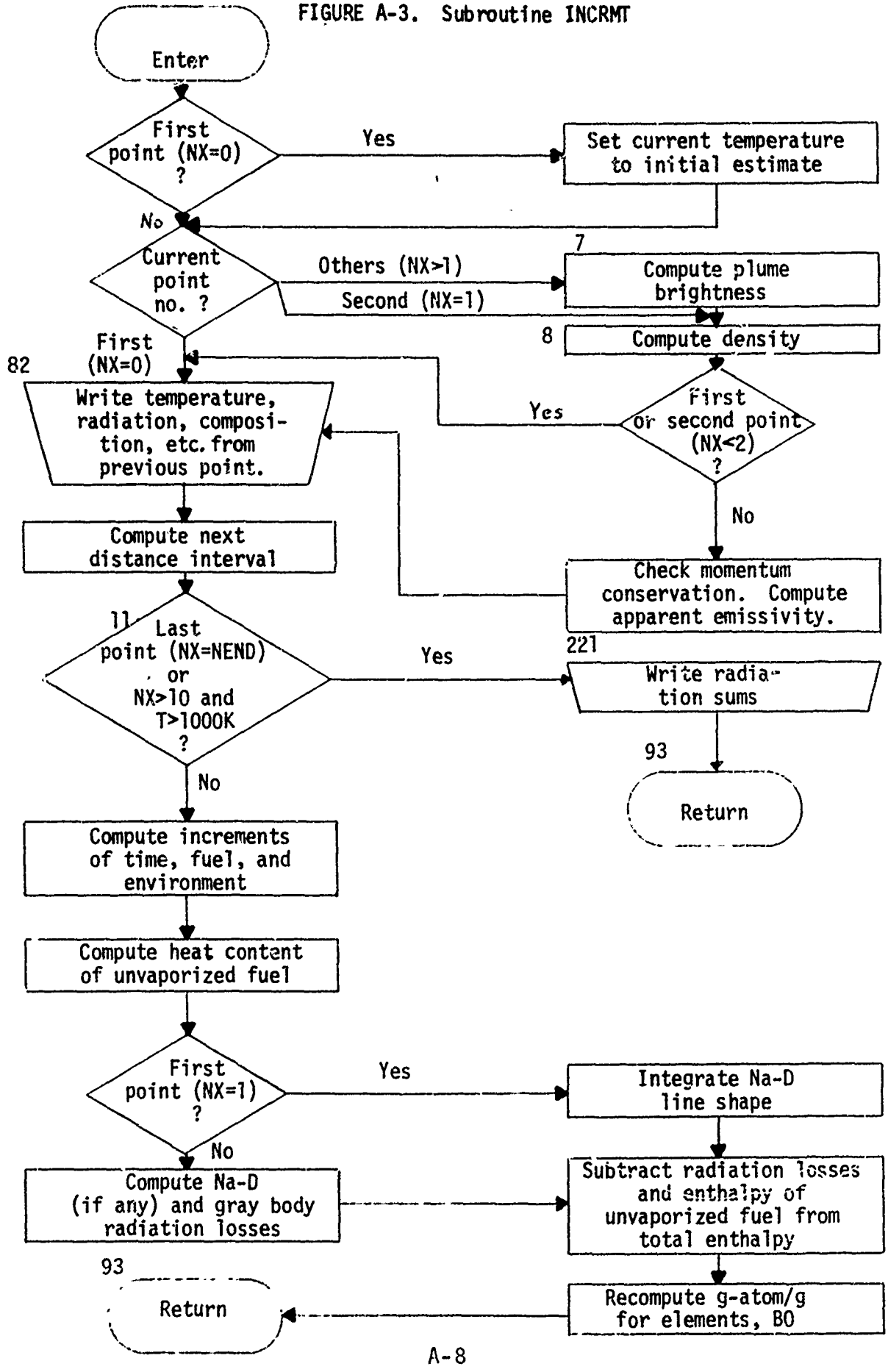

of the more important variables introduced, and their definitions, is given in Table A-2. Table A-3 shows a listing of input and output from an actual run.

Following the control cards, the usual cards for the NASA program must be furnished, beginning with the THERMO data cards if the thermodynamic data is not furnished on tape. The format is unchanged from that described by Gordon and McBride, and the details may be found there or may be discerned from the example given below.

Because of the modifications there are a few special restrictions on the input furnished here:

1. The first reactant card must be for the fuel, assumed to be an element in particle form.

2. The last reactant card is for the intended ambient environment. All elements listed on this card must be listed on one of the previous cards (in order to avoid a singular matrix at the first point), though this need be only in a minute quantity. For example, if the environment contains argon, one of the cards before the last must list a non-zero amount of argon.

3. All reactants must be listed as fuels, "F".

4. On the "namelists" card only the "HP" option is to be used. IONS=T may not be used. "FPCT=T, MIX=100." are to be included.

Immediately following the "namelists" input card is a card with the word "CONDitions", followed by a card listing the assumed combustion conditions--flare diameter and burning rate, etc. These conditions and the input formats are listed in statements numbered 32 and 31, resp. in

TABLE A-2
MODIFICATIONS TO NASA PROGRAM

Additions or changes are indicated by brackets in A throug C.

A. Subroutine SEARCH

```
      COMMON/INDX/ IDEBUG,CONVG,TP,HP,SP,ISV, NPP, MOLES,NP,NT,NPT,NLM,
     1  ,NS,KMAT,IMAT,IQ1,NOF,NOMIT,IP,NEWR,NSUB,NSUP,ITM,CPCVFR,CPCVEQ
     2 ,IONS,NC,NSERT,JSOL,JLIQ,KASE,NREAC,IC,JS1,VOL,SHOCK,IT,NFZ,CALCH
     3 ,IQSAVE,LSAVE,ISUP,ISUB,ITNUM,NX,NEND,THF ,WI,WF,WFA,ESTR,BSTR
     4 ,RATE, DX, TI ,KRON, DXF, FLOWZ,XZRO,A3, WT(14), AZRO, L12
     5,NA,NMG,NCF,LLB(15),NOUT(10),KSP,BL(5,2),KB,LLA(15,25,2)

C  CONDENSED SPECIES
C
      NC= NC+1
      TEMP(NC,1)= T1
      TEMP(NC,2)= T2
      IF (MT(1).NE.NAME(1,1)) GO TO 12
   11 IF (MT(2).NE.IZERO.AND.MT(2).NE.JZERO) GO TO 12
      NCF = NC
      NPG = NS
   12 CONTINUE
```

B. Subroutine EQLBRM

```
    1 SINGC = .FALSE.
      IF(NX.EQ.0) CALL INCRMT
      PIE = 0.


   43 IF (.NOT.CONVG)  GO TO 62
      SUM = ENN
      CALL INCRMT
      IF(NX.EQ.NEND) GO TO 1000
      IF(NX.GT.10.AND.TT.LT.1000) GO TO 1000
      GO TO 1
   62 CALL MATRIX
```

TABLE A-2 (Cont.)

C. Subroutine THERMP


```
      COMMON/MISC/ENN,SUMN,TT,SO,ATOM(3,101),LLMT(15),BO(15),BOP(15,2)
     1 ,T0,TLOW,THIG,THIGH,PP,CPSUM,OF,EQRAT,FPCT,R,RR,HSUBO,AC(2),AM(2)
     2 ,HPP(2),RH(2), VMIN(2),VPLS(2),WP(2),DATA(22),NAME(15,5)
     3 ,ANUM(15,5),PECWT(15),ENTH(15),FAZ(15),RTEMP(15),FOX(15),DENS(15)
     4 ,RHOP,RM(15),TLN,CR,OXF(15),ENNL,ENSAVE,ENLSAV ,TRACE,SIZE,BD(5)
      COMMON/INDX/ IDEBUG,CONVG,TP,HP,SP,ISV, NPP, MOLES,NP,NT,NPT,NLM
     1  ,NS,KNAT,IMAT,IQ1,NOF,NOMIT,IP,NEWR,NSUB,NSUP,ITM,CPCVFR,CPCVEQ
     2 ,IONS,NC,NSERT,JSOL,JLIQ,KASE,NREAC,IC,JS1,VOL,SHOCK,IT,NFZ,CALCH
     3 ,IQSAVE,LSAVE,ISUP,ISUB,ITNUM,NX,NEND,TWF ,WI,WF,WFA,CNAD, CBB
     4 ,POWR, DX, TI ,KRON, DTL, FLOWZ,XZRO,A3, WT(14), DZRO, L12
     5 , NA, NMG, NCF, LLB(15), NOUT(10), KSP, BL(5,2), KB, LLA(15,25,2)
      COMMON/OUPT/FMT(30),FP(4),FT(4),FH(4),FS(4),FM(4),FV(4),FD(4)
     1  ,FG(4),FG(4),FB,FMT13,F1,F2,F3,F4,F5,FL(4),FMTI9,FA1,FA2
     2  ,FR1,FC1,FN(4),FR(4),FA(4),FI(4),FMT9X,FO
C
      EQUIVALENCE (K,ISV ),(VL,P),(UV,HP),(TP,TV),(SP,SV)
C
      DATA FUU/4HU, C/
      DATA COND/4HCOND/,BAND/4HBAND/,SPEC/4HSPEC/,BLANK/1H /
      DATA SPCN(2)/4HNA  /,OMIT/4HOMIT/
C
      DO 902 IT=1,NT
      TT = T(IT)
C     BEGINNING OF MODIFICATIONS,INITIALIZATIONS,
      DO 215 I=1,NLM
      M = 0
      DO 213 J=1,NREAC
      DO 212 K=1,5
      IF (NAME(J,K).NE.LLMT(I)) GO TO 212
      M = M+1
      LLA(I,M,1) = J
      LLA(I,M,2) = K
  212 CONTINUE
  213 CONTINUE
      LLB(I) = M
  215 CONTINUE
      READ (5,31)
   30 KSP = 0
      KB = 0
      DO 52 I=1,5
      BL(I) = 0
      DO 52 J=1,2
   52 BL(I,J) = 0
      DO 58 I=1,9
      NOUT(I) = 0
      DO 58 J=1,2
   58 SPC(I,J) = 0
C     READ NEXT SET OF BURNING CONDITIONS,
      READ  (5,31) DZRO,DEN ,TI,BRT,THETA,WI,WF, TWF,POWR,WFA,CNAD,L12
     1 ,CBB, KRON,DX,DTL,NEND ,PLOTT
      IF (NEND.EQ.0) GO TO 40
```

TABLE A-2 (Cont.)

C. Subroutine THERMP (Cont.)

```
      WRITE (6,32)
   32 FORMAT (87H1 DZRO  DEN  TI   BRT THETA WI  WF  TWF POWR WFA CNAD L
     112 CBR  KRON DX DXF NEND PLOTT    )
      WRITE (6,31) DZRO,DEN ,TI,BRT,THETA,WI,WF, TWF,POWR,WFA,CNAD,L12
     1 ,CBR, KRON,DX,DTL,NEND ,PLOTT
   31 FORMAT (1H ,F5.2,F5.2,F5.0,F5.2,F5.3,F4.1,F5.1,F4.2,F4.1,F6.0,F4.1
     1 ,I3,E8.1,I2,F4.1,F4.0,I4,L2)
   50 READ (5,51) ROUTE
   51 FORMAT (A4)
      IF (ROUTE.EQ.COND.OR.ROUTE.EQ.BLANK) GO TO 79
      IF (ROUTE.EQ.BAND) GO TO 53

C     READ SPECIES FOR PRINTOUT OF EQUILIBRIUM CONCENTRATIONS
      READ (5,33)((SPC(I,J),J=1,2),I=1,9)
   33 FORMAT (18A4)
      DO 37 I=1,9
      IF (SPC(I,1)) 38, 38, 34
   34 DO 36 J=1,150
      IF (SUB(J,1).EQ.SPC(I,1).AND.SUB(J,2).EQ.SPC(I,2)) GO TO 35
   36 CONTINUE
      SPC(I,2) = OMIT
   35 NOUT(I) = J
   37  CONTINUE
      KSP = I
      GO TO 50
   38 KSP = I-1
      GO TO 50

C     READ WAVELENGTH BANDS TO BE CALCULATED.
   53 READ (5,54) ((BL(I,J),J=1,2),I=1,5)
   54 FORMAT (10F5.2)
      WRITE(6,57) ((BL(I,J),J=1,2),I=1,3)
   57 FORMAT (14HO BAND LIMITS ,/,3(F9.2,4H TO ,F5.2))
      DO 55 I=1,5
      IF(BL(I,1).EQ.0) GO TO 56
   55 CONTINUE
      KB = I
      GO TO 50
   56 KB = I-1
      GO TO 50
   79 IF (KSP+KB.GT. 9) KSP= 9-KB

C     TABLE HEADINGS.
      WRITE (6,80)
      WRITE (6,81)((SPC(I,J),J=1,2),I=1,KSP)
   80 FORMAT(105HO PT   DIST TIME(S) TEMP   RAD     LUM    BRIGHT  SODIUM
     1  EFF        MOLE FRACTIONS,  BAND ENERGIES                  )
   81 FORMAT (55H      (CM)           (K)  CAL/R   CDS/G   CD/CM2  CAL/R
     1 ,8X, 18A4)

C     MORE INITIALIZATIONS.
      NA = 0
      DO 72 I=1,NS
      IF (SUB(I,1).EQ.SPCN(2)) NA=I
   72 CONTINUE
```

TABLE A-2 (Cont.)

C. Subroutine THERMP (Cont.)


```
      W = 0
      NLESS = NPEAC-1
      DO 83 I=1,NLESS
   83 W=W+PECNT(I)
      DO 84 I=2,NLESS
   84 WT(I) = 100*PECNT(I)/W
      XZRO = DZRO/2/TAN(THETA)
      FLOWZ = .785398*DZRO**2*BRT*DEN
      NX = 0

      CALL EQLBRM

      IF(.NOT.PLOTT) NPLPTS=0
      IF(.NOT.PLOTT) GO TO 30
      CALL PLOTS(BUF,63,20)
      CALL FACTOR(2.)
      EMARAY(1) = EMARAY(2)
      CALL PLOT(0.,-11.,-3)
      CALL PLOT(1.5,9.,-3)
      CALL SCALE(T2ARAY,5.,NPLPTS,1)
      CALL AXIS(0.,0.,19HTEMPERATURE, DEGS K, 19,5.,0.,T2ARAY(NPLPTS
     1 +1),T2ARAY(NPLPTS+2))
      CALL SCALE(XCARAY,7.,NPLPTS,1)
      CALL AXIS(0.,0.,12HDISTANCE, CM,-12,7.,-90.,XCARAY(NPLPTS+1),
     1 XCARAY(NPLPTS+2))
      CALL SCALE(EMARAY,5.,NPLPTS,1)
      CALL AXIS(0.,-7.,27H  LOG(LUMINANCE), CD/SQ-CM   ,-27,05.,0.,
     1 EMARAY(NPLPTS+1),EMARAY(NPLPTS+2))
      XCARAY(NPLPTS+2)=XCARAY(NPLPTS+2)
      CALL LINE(T2ARAY,XCARAY,NPLPTS,1,0,0)
      CALL LINE(EMARAY,XCARAY,NPLPTS,1,0,0)
      CALL PLOT(7.,-10.,-3)
      PLT=0.
      NPLPTS=0
      GO TO 30
   40 WRITE (6,41) NX
   41 FORMAT (I5)

C     CONTINUE WITH UNMODIFIED SUBROUTINE
      IF(TT.NE.0.)  GO TO 800
      IF(NPT.EQ.0)  GO TO 1000
  800 K = 0
```

TABLE A-2 (Cont.)

D. Subroutine INCRMT

```
      SUBROUTINE INCRMT
      DIMENSION DIAM( 5),T( 5 ),TIME( 5 ),RNAD( 5 ),RBB ( 5 ), CONC(10)
     1 ,EL1(5),EL2(5),RHO(5),SRNAD(5),SRBB(5),GMR(14)
     2 , SS (5),                    BBE(18,2), BU(11)
      LOGICAL HP,SP,TP,        CONVG,NEWR,IONS,MOLES,EQL,FROZ,VOL
      COMMON/PLOTC/ PLPTS,XCARAY(202),T2ARAY(202),EMARAY(202) ,BUF(63)
      COMMON/PLTR/ PLT
      COMMON/MISC/ENN,SUMN,TT,SO,ATOM(3,101),LLMT(15),BO(15),BOP(15,2)
     1 ,TM,TLOW,TMID,THIGH,PP,CPSUM,OF,EQRAT,FPCT,R,RR,HSUBO,AC(2),AM(2)
     2 ,HPP(2),RH(2), VMIN(2),VPLS(2),WP(2),DATA(22),NAME(15,5)
     3 ,ANUM(15,5),PECWT(15),ENTH(15),FAZ(15),RTEMP(15),FOX(15),DENS(15
     4 ,RHOP,RMW(15),TLN,CR,OXF(15),ENNL,ENSAVE,ENLSAV ,TRACE,SIZE,BD(5)
      COMMON/INDX/ IDEBUG,CONVG,FP,HP,SP,ISV, NPP, MOLES,NP,NT,NPT,NLM
     1  ,NS,KMAT,IMAT,IQ1,NOF,NOMIT,IP,NEWR,NSUB,NSUP,ITM,CPCVFR,CPCVEQ
     2 ,IONS,NC,NSERT,JSOL,JLIQ,KASE,NREAC,IC,JS1,VOL,SHOCK,IT,NFZ,CALCH
     3 ,IQSAVE,LSAVE,ISUP,ISUB,ITNUM,NX,NEND,TWF ,WI,WF,WFA,CNAD, CBB
     4 ,POWR, DX, TI ,KRON, DTL, FLOWZ,XZRO,A3, WT(14), DZRO, L12
     5 , NA, NMG, NCF, LLB(15), NOUT(10), KSP, BL(5,2), KB, LLA(15,25,2)
      COMMON/SPECES/COEF(2,7,150),S(150),EN(150,13),ENLN(150),HO(150)
     1,DELN(150),A(15,150),SUB(150,3),IUSE(150),TEMP(50,2),SLN(150)
      DATA    BBE                          /1800.,1900.,2000.,2100.,2200.
     1 ,2300.,2400.,2500.,2600.,2700.,2800.,2900.,3000.,3100.,3200.
     2 ,3300.,3400.,3500.,    .001,.0017,.00255, .0034, .0052, .007, .009
     3 , .012, .015, .018, .0215, .0255, .03, .0345, .0395, .044, .049
     4 , .055 /
      OPTF(A,B)=((A+1.)**(-1./(A*B*B)))*(1.-((A+1.)**(-1./(B*B))))
      T(1)= TT
      IF(NX.EQ.0) TT=TI

C     RELOCATION OF STORED QUANTITIES
      DO 2  I=1,4
      T   (6-I) = T   (5-I)
      TIME(6-I) = TIME(5-I)
      RNAD(6-I) = RNAD(5-I)
      RBB (6-I) = RBB (5-I)
      SRNAD(6-I) = SRNAD(5-I)
      SRBB(6-I) = SRBB(5-I)
      RHO (6-I) = RHO (5-I)
      DIAM(6-I) = DIAM(5-I)
    2 CONTINUE

C     FLAME BRIGHTNESS, SYSTEM DENSITY, MOMENTUM CONSERVATION, GRAY
C       BODY EFFICIENCY.
      IF (NX-1) 82, 8, 7
    7 BRIT = 100.*TLUM*RHO(3)*DIAM(2)/(100+WT(NREAC))/(TIME(2)-TIME(3))
    8 RHO(2) = .01219*PP/ENN/TT*(100+WT(NREAC))/W
      IF (NX.LT.2) GO TO 82
      RHO2 = PP*RMW(NREAC)/R/T(2)
      CON = (RHO2+RHO(2))/RHO2*WFA*POWR*(XC/200)**(POWR-1)/2E4-(1+WT
     1 (NREAC)/100)*2/(XC+XZRO)
      IF (CON.GT.0) WRITE (6,84)
   84 FORMAT (34H FORWARD MOMENTUM CHANGE POSITIVE  )
      EFF = 3.64E13*RBB(2)*RHO(2)*DIAM(2)/TT**4/(TIME(2)-TIME(3))/
     1 (100+WT(NREAC))

C     PRINTOUT OF RESULTS FOR LAST POINT
      DO 9 I=1,KSP
```

TABLE A-2 (Cont.)

D. Subroutine INCRMT (Cont.)

```
      NF = NCOT(I)
    9 C  C(I) = RN(NF,1)
   82 WRITE (6,83) NX,XC, TIME(2), T(2), RBB(2), TLUM, BRIT, RNAD(2),EFF
     1 , (CC C(I),I=1,KSP), (BD(I),I=1,KB)
   83 FORMAT (1HO,I3, F6.1, F8.4, F7.1, F6.1, F8.1, E9.2, F7.3, F5.3
     1 ,9F8.5)
      IF(PLT.EQ.0.) GO TO 42
      NPLPTS=NPLPTS+1
      XCARAY(NPLPTS)=XC
      T2ARAY(NPLPTS)=T(2)
      EMARAY(NPLPTS) = ALOG10(BRIT)
      IF(BRIT.LE..0001 ) EMARAY(NPLPTS)=-4.
   42 PLT=1.

C     READJUSTMENT OF INTERVAL BETWEEN POINTS.
      IF (NX.LT.6) GO TO 12
      RDT = ABS(T(5)/6+T(4)/3+T(3)/2-T(2))*.6 /DTL
      DX = DX*(1.3+.7*RDT)/(1+RDT)
   12 NX = NX+1
   13 XC = XC+DX
      IF (NX-1) 10,10,11
   10 XC=0
      STLUM = 0
      SBL   = 0
      DO 34 I=1,KB
   34 SBD(I) = 0

C     EXIT ON COMPLETION OF CALCULATIONS.
   11 IF(NX.EQ.NEND) GO TO 221
      IF(NX.GT.10.AND.TT.LT.1000) GO TO 221

C     PLUME DIAMETER, FLIGHT TIME, AND WEIGHTS OF FUEL AND ENVIRONMENT
C       FOR NEXT POINT.
      DIAM(1) = DZRO*(XC+XZPO)/XZRO
      IF (NX-1) 221, 15, 16
   15 TIME(1) = 0
      GO TO 17
   16 TIME(1) = TIME(2)+DX*RHO(2)*78.54/FLOWZ/(100+WT(NREAC))*DIAM(1)**2
   17 WT(1) = WI+(WF-WI)*(TIME(1)/TWF)
      IF( T(1).GT.WF) WT(1)=WF
      WT(NREAC) = WFA*(XC/200.)**POWR
      W = 0
      DO 20 I = 1,NREAC
   20 W = WT(I)+W

C     HEAT CONTENT OF UNVAPORIZED FUEL

      HMG = 0
      TEP = TT
      LMG = NMG
      IF (TT.LT.TEMP(NCF,1)) LMG=LMG-1
      IF (TT.GT.TEMP(NCF,2)) TEP=TEMP(NCF,2)
      DO 30 I=1,5
      II = 6-I
   30 HMG = (HMG+COEF(2,II,LMG)/II)*TEP
      HMG = HMG+COEF(2,6,LMG)
```

TABLE A-2 (Cont.)

D. Subroutine INCRMT (Cont.)

```
C     INITIAL INTEGRATION OF LINE SHAPE.
      IF(NA.GT.1) GO TO 35
      XL2=FLOAT(L12)
      RAD1 = OPTF(XL2,.2)
      XWAV = -.2
      DO 31 I=1,13
      XWAV = XWAV+.4
   31 RAD1 = RAD1+4*OPTF(XL2,XWAV)
      XWAV = 0
      DO 32 I=1,12
      XWAV = XWAV+.4
   32 RAD1 = RAD1+2*OPTF(XL2,XWAV)
      RAD1 = RAD1*.2/3+ALOG(L12+1.)/27.04
      RAD1 = 2*RAD1
      SRNAD(1) = 0
      SRBB(1) = 0
      GO TO 37

C     RADIATION COMPUTATIONS FOR NEXT POINT.
   35 IF (NA  .EQ.0) GO TO 36
      RNAD(1) = 3.75E5*W*EXP(-24416/TT)*(EN(NA,1)*ENN*TT**.5/DIAM(1)
     1 /ALOG(L12+1.))**.5*RAD1*CNAD*(TIME(1)-TIME(2))
      SRNAD(1) = SRNAD(2)+RNAD(1)
   36 RBB(1) = (TIME( 1)-TIME( 2)  )*CBB   *TT**4
      SRBB(1) = SRBB(2)+RBB(1)
      IF (TT.GE.BBE(1,1)) GO TO 60
      BBL    = 0
      GO TO 64
   60 DO 61 I=2,17
      IF (TT.LE.BBE(I,1)) GO TO 63
   61 CONTINUE
      WRITE (6,62)
   62 FORMAT (60H TEMPERATURE EXCEEDS RANGE OF LUMINOUS EFFICIENCY TABLE
     1       )
   63 P = (TT-BBE(I,1))/100
      PA = P+1
      PM = P-1
      BBL    = (P*PM*BBF(I-1,2)/2-PA*PM*BBE(I,2)+P*PA*BBE(I+1,2)/2)*RBB
     1 (1)
   64 SBL    = SBL   +BBL
      IF (KB.EQ.0) GO TO 49
      DO 45 I=1,KB
      BU(11) = 1.4388325E4/BL(I,2)/TT
      BU( 1) = 1.4388325E4/BL(I,1)/TT
      DO 46 J=2,10
   46 BU(J) = BU(1)+.1*(J-1)*(BU(11)-BU(1))
      B1 = BU(1)**3/(EXP(BU(1))-1)  +BU(11)**3/(EXP(BU(11))-1)
      DO 47 J=2,10,2
   47 B1 = B1+4*BU(J)**3/(EXP(BU(J))-1)
      DO 48 J=3,9,2
   48 B1 = B1+2*BU(J)**3/(EXP(BU(J))-1)
      BD(I) = B1/3.*.15399*(BU(2)-BU(1))*TT**4*CBB    *(TIME(2)-TIME(1))
   45 SBD(I)= SBD(I)+BD(I)
   49 CONTINUE
      TLUM = 330*RNAD(1)+450*BBL
      STLUM = STLUM+TLUM
```

TABLE A-2 (Cont.)

D. Subroutine INCRMT (Cont.)


```
C       ENTHALPY FOR NEXT POINT.
   37 HSUBO = -.041144*HMG*(100+WT(NREAC)-W)-100.*(SRNAD(1)+SRBB(1))*
     1 RSQN
        DO 38 I=2,NREAC
   38 HSUBO = HSUBO+WT(I)*ENTH(I)/RMW(I)/R
        HSUBO = HSUBO/W

C       OTHER QUANTITIES FOR NEXT POINT.
        HPP(2)=0.
        VPLS(2)=0.
        VMIN(2)=0.
        AM(2)=0.

        DO 220 N=1,NREAC
        PECWT(N) = WT(N)/W
        GMR(N) = PECWT(N)/RMW(N)
        HPP(2)=HPP(2)+ ENTH(N)*PECWT(N)/(RMW(N)*R)
        AM(2)=AM(2)+PECWT(N)/RMW(N)
  220 CONTINUE
        AM(2) = 1./AM(2)
        DO 215 I=1,NLM
        BOP(I,2) = 0
        IL = LLB(I)
        DO 213 M=1,IL
        LL1 = LLA(I,M,1)
        LL2 = LLA(I,M,2)
        BOP(I,2) = BOP(I,2)+GMR(LL1)*ANUM(LL1,LL2)
  213 CONTINUE
        BO(I) = BOP(I,2)
  215 CONTINUE

        NEWR = .FALSE.
   93 RETURN

C       FINAL PRINTOUT.
  221 SRNADL = 330*SRNAD(1)
        SBL = 450*SBL
        SRNAD(1) = R*SRNAD(1)
        SRBB(1) = R*SRBB(1)
        DO 90 I=1,KB
        BL1(I) = BL(I,1)
        BL2(I) = BL(I,2)
   90 SBD(I) = R*SBD(I)
        WRITE (6,94) SRNAD(1), SRNADL, SBL, STLUM, SRBB(1), (BL1(I),BL2(I)
     1 ,SBD(I),I=1,KB)
   94 FORMAT (17H SODIUM-D ENERGY  F8.3,6H CAL/G/21HOSODIUM-D LUMINOSITY
     1  F10.2,9H CD-SEC/G /21H GRAY BODY LUMINOSITY F10.2,9H CD-SEC/G /
     2 21H TOTAL LUMINOSITY     F10.2,9H CD-SEC/G /24HOTOTAL GRAY BODY E
     3NERGY  F8.3,6H CAL/G/24HOBAND GRAY BODY ENERGIES /5(F4.1,1H- F4.1,
     4 F10.3,6H CAL/G/))
        GO TO 93
        END
```

TABLE A-3. INPUT AND OUTPUT OF A SAMPLE RUN

```
REACTANTS
MG1.0                                                  58.      0.0      S298.15  F 1.74
NA1.      N 1.      O 3.                               17.5    -111540. S298.15  F 2.26
C 5.A5    H 8.36    O 1.15    N .3                     4.5     -53900.  L298.15  F
N 8.26    O 2.                                         0.       0.0     G298.15  F

INSERT          MGO(S)          NA2O(S)
OMIT            CN              NH              CH2
OMIT            CHN             C2O             NH2             CH3
OMIT            C2H             C               CH              C2
OMIT            CH2O            CN2             C2H2            C2H4
OMIT            C2N             C3              C4              C5
NAMELISTS
 SINPT2  HP=T, P= 1.   , FPCT=T, MIX = 100.    $
CONDITIONS
 10.0 1.7  1000. .25  .3   2.  50.   .1  1.  200. 2.  10 2.6E-11 1 .2  60. 100 T
SPECIES
C(S)    CO      CO2     H2O     NA      MGO
BANDS
1.5  2.5  2.5  3.5

REAC
```

```
REACTANTS
MG  1.0000      -0.0000     -0.0000     -0.0000     -0.0000    23.000000        0.00  S  298.150  F    1.74000
NA  1.0000  N   1.0000  O   3.0000     -0.0000     -0.0000    37.500000  -111540.00  S  298.150  F    2.26000
C   5.8300  H   8.3600  O   1.1500  N   .3000     -0.0000     4.300000   -53900.00  L  298.150  F   -0.00000
N   8.2600  O   2.0000     -0.0000     -0.0000     -0.0000     0.000000        0.00  G  298.150  F   -0.00000
INSERT          MGO(S)          NA2O(S)
OMIT            CN              NH              CH2
OMIT            CHN             C2O             NH2             CH3
OMIT            C2H             C               CH              C2
OMIT            CH2O            CN2             C2H2            C2H4
OMIT            C2N             C3              C4              C5
NAMELISTS

BAD CARD: SINPT2  HP=T, P= 1.   , FPCT=T, MIX = 100.    $

TOO FEW CONSTANTS FOR UNSUBSCRIPTED ARRAY
ERROR NUMBER   0049 DETECTED BY NAMINP  AT ADDRESS 000530
CALLED FROM TAPR    AT  LINE 0177

BAD CARD: SINPT2  HP=T, P= 1.   , FPCT=T, MIX = 100.    $

TOO FEW CONSTANTS FOR UNSUBSCRIPTED ARRAY
ERROR NUMBER   0049 DETECTED BY NAMINP  AT ADDRESS 000530
CALLED FROM TAPR    AT  LINE 0177

SINPT2

KASE    = 0,

T       = 0.0,  0.0,  0.0,  0.0,  0.0,  0.0,  0.0,  0.0,  0.0,  0.0,  0.0,      0.0,  0.0,  0.0,  0.0,  0.0,
          0.0,  0.0,  0.0,  0.0,  0.0,  0.0,  0.0,  0.0,  0.0,  0.0,

P       = 0.1E+01,  0.0,  0.0,  0.0,  0.0,  0.0,  0.0,  0.0,  0.0,  0.0,  0.0,  0.0,  0.0,  0.0,  0.0,  0.0,
          0.0,  0.0,  0.0,  0.0,  0.0,  0.0,  0.0,  0.0,  0.0,  0.0,

PSIA    = F,

MMHG    = F,

NSQM    = F,

V       = 0.0,  0.0,  0.0,  0.0,  0.0,  0.0,  0.0,  0.0,  0.0,  0.0,  0.0,      0.0,  0.0,  0.0,

RHO     = 0.1E+01,  0.0,  0.0,  0.0,  0.0,  0.0,  0.0,  0.0,  0.0,  0.0,  0.0,  0.0,  0.0,  0.0,  0.0,  0.0,
          0.0,  0.0,  0.0,  0.0,  0.0,  0.0,  0.0,  0.0,  0.0,  0.0,

ERATIO  = F,

OF      = F,

FPCT    = T,

FA      = F,

MIX     = 0.1E+03,  0.0,  0.0,  0.0,  0.0,  0.0,  0.0,  0.0,  0.0,  0.0,  0.0,  0.0,  0.0,  0.0,  0.0,  0.0,

TP      = F,

HP      = T,

SP      = F,

TV      = F,

UV      = F,

SV      = F,

RKT     = F,

SHOCK   = F,

DETN    = F,
```

TABLE A-3 (cont.)

21	6.3	.0190	1911.4	.4	1.6	.11E+02	.004	.084	0.00000	.00003	.00424	.00082	.00233	.00000	.19092	.07644
22	6.8	.0202	2043.4	.5	2.4	.16E+02	.006	.082	0.00000	.00004	.00414	.00079	.00266	.00000	.16432	.08132
23	7.2	.0213	2099.5	.5	3.0	.24E+02	.009	.081	0.00000	.00007	.00404	.00096	.00297	.00000	.18388	.08677
24	7.7	.0224	2154.7	.6	5.3	.34E+02	.013	.080	0.00000	.00011	.00393	.00111	.00327	.00000	.20308	.09298
25	8.2	.0234	2207.4	.6	7.5	.48E+02	.019	.079	0.00000	.00016	.00381	.00125	.00356	.00000	.22491	.09994
26	8.7	.0247	2259.2	.7	10.6	.65E+02	.027	.078	0.00000	.00023	.00367	.00138	.00382	.00000	.24772	.10767
27	9.2	.0257	2309.6	.8	14.5	.85E+02	.037	.077	0.00000	.00032	.00351	.00148	.00405	.00000	.27252	.11586
28	9.8	.0271	2359.2	.9	19.5	.11E+03	.050	.076	0.00000	.00043	.00334	.00157	.00425	.00000	.30201	.12512
29	10.3	.0283	2407.9	1.0	25.7	.14E+03	.067	.075	0.00000	.00057	.00314	.00164	.00441	.00000	.33346	.13590
30	10.8	.0294	2456.0	1.1	33.7	.17E+03	.088	.075	0.00000	.00072	.00292	.00168	.00455	.00001	.36823	.14649
31	11.4	.0309	2503.4	1.2	43.7	.21E+03	.114	.074	0.00000	.00088	.00270	.00170	.00466	.00001	.40668	.15881
32	12.0	.0322	2549.9	1.4	56.0	.26E+03	.147	.073	0.00000	.00105	.00246	.00171	.00474	.00002	.44925	.17239
33	12.6	.0336	2595.4	1.6	71.1	.31E+03	.187	.073	0.00000	.00123	.00221	.00169	.00479	.00003	.49631	.18730
34	13.2	.0351	2639.6	1.7	89.4	.38E+03	.235	.072	0.00000	.00141	.00197	.00166	.00483	.00004	.54823	.20407
35	13.9	.0367	2681.8	2.0	111.5	.43E+03	.295	.072	0.00000	.00158	.00173	.00161	.00484	.00007	.60859	.22286
36	14.6	.0383	2721.5	2.2	138.2	.49E+03	.366	.071	0.00000	.00174	.00151	.00154	.00484	.00010	.67636	.24436
37	15.3	.0401	2758.2	2.5	170.4	.56E+03	.452	.071	0.00000	.00188	.00130	.00146	.00482	.00013	.75517	.26950
38	16.1	.0420	2791.3	2.9	209.6	.63E+03	.557	.070	0.00000	.00200	.00111	.00137	.00479	.00018	.84888	.29943
39	17.0	.0441	2820.6	3.3	257.5	.73E+03	.685	.070	0.00000	.00209	.00094	.00128	.00474	.00023	.96298	.33644
40	17.9	.0464	2845.8	3.8	316.9	.77E+03	.845	.070	0.00000	.00217	.00079	.00117	.00467	.00029	1.10519	.38315
41	18.9	.0493	2866.8	4.5	392.0	.83E+03	1.046	.070	0.00000	.00222	.00065	.00106	.00459	.00039	1.28648	.44287
42	20.1	.0521	2883.5	5.3	478.6	.88E+03	1.303	.069	0.00000	.00226	.00053	.00095	.00449	.00040	1.52280	.52121
43	21.4	.0557	2895.6	6.5	616.2	.93E+03	1.647	.069	0.00000	.00227	.00042	.00083	.00437	.00045	1.83855	.62644
44	23.0	.0601	2902.5	8.1	789.4	.98E+03	2.113	.068	0.00000	.00225	.00033	.00070	.00423	.00048	2.27357	.77218
45	25.0	.0657	2902.9	10.3	1034.0	.99E+03	2.773	.068	0.00000	.00221	.00025	.00058	.00405	.00049	2.89855	.98265
46	27.5	.0731	2894.2	13.7	1400.4	.99E+03	3.765	.068	0.00000	.00214	.00017	.00044	.00384	.00046	3.85648	1.30724
47	30.6	.0833	2872.3	18.1	1856.3	.97E+03	5.002	.067	0.00000	.00204	.00011	.00032	.00359	.00040	5.09567	1.73123
48	34.2	.0954	2834.3	21.8	2209.0	.91E+03	5.969	.067	0.00000	.00191	.00006	.00020	.00332	.00030	6.20148	2.11943
49	38.2	.1097	2817.5	24.0	2246.1	.79E+03	6.060	.067	0.00000	.00183	.00003	.00018	.00316	.00026	6.91290	2.38739
50	42.8	.1277	2812.9	29.6	2821.1	.76E+03	7.691	.069	0.00000	.00174	.00006	.00018	.00306	.00024	8.57700	2.97603
51	48.2	.1530	2757.4	41.2	3334.5	.74E+03	9.476	.054	0.00000	.00170	.00006	.00018	.00295	.0002111.96808		4.15809
52	54.3	.1890	2754.2	57.3	4656.6	.76E+03	12.440	.080	0.00000	.00163	.00005	.00017	.00282	.0001916.73978		5.84173
53	62.1	.2374	2707.9	73.5	5670.0	.72E+03	14.553	.068	0.00000	.00156	.00004	.00014	.00270	.0000921.74828		7.66291
54	69.8	.2976	2629.6	84.3	5484.8	.63E+03	14.522	.077	0.00000	.00150	.00003	.00011	.00258	.0000425.47107		9.12788
55	77.3	.3679	2539.7	87.2	4727.0	.51E+03	12.441	.087	0.00000	.00145	.00002	.00008	.00247	.0000227.10381		9.65732
56	84.4	.4457	2450.8	84.3	3668.3	.39E+03	9.600	.094	0.00000	.00139	.00002	.00006	.00238	.6000126.9890810.22253		
57	91.2	.5300	2363.0	79.1	2719.0	.29E+03	7.105	.102	0.00000	.00134	.00002	.00007	.00229	.0000026.0429910.19027		
58	97.6	.6202	2280.9	73.3	1968.3	.21E+03	5.146	.110	0.00000	.00126	.00006	.00010	.00220	.0000024.7366710.01243		
59	103.4	.7129	2076.9	64.4	1119.3	.12E+03	2.991	.137	0.00000	.00110	.00017	.00037	.00207	.0000021.16306	9.03927	
60	108.5	.8049	1979.1	45.3	474.5	.57E+02	1.238	.135	0.00000	.00094	.00031	.00048	.00195	.0000018.19239	7.46273	
61	113.1	.8951	1901.0	38.0	243.3	.37E+02	.621	.135	0.00000	.00076	.00045	.00056	.00183	.0000012.19470	6.56226	
62	117.4	.9863	1841.0	33.9	144.4	.29E+02	.365	.136	0.00000	.00060	.00060	.00058	.00172	.0000011.16883	5.73619	
63	121.6	1.0809	1790.0	28.3	93.9	.13E+02	.241	.139	0.00000	.00043	.00074	.00055	.00159	0.0000010.21828	5.46350	
64	125.9	1.1838	1745.4	27.3	56.5	.73E+01	.171	.142	0.00000	.00027	.00088	.00052	.00144	0.00000	9.77022	5.41485
65	130.2	1.2952	1703.9	27.1	41.7	.51E+01	.126	.145	0.00000	.00012	.00100	.00049	.00123	0.00000	9.63856	5.92193
66	134.9	1.4209	1672.1	27.7	31.2	.35E+01	.093	.148	0.00000	.00003	.00108	.00030	.00090	0.00000	9.76339	5.76847
67	139.7	1.5647	1632.9	29.2	22.8	.23E+01	.069	.155	0.00000	.00000	.00108	.00008	.00046	0.0000010.21245	6.20207	
68	145.0	1.7269	1589.6	30.5	13.1	.12E+01	.040	.174	0.00000	.00000	.00106	.00005	.00022	0.0000010.31782	6.60328	
69	150.3	1.9115	1543.8	28.7	5.5	.44E+00	.017	.184	0.00000	.00000	.00104	.00008	.00008	0.00000	9.64336	6.41023
70	155.7	2.1073	1496.6	26.2	1.8	.16E+00	.006	.185	0.00000	.00000	.00102	.00008	.00003	0.00000	8.90109	6.01396
71	161.1	2.3205	1423.4	25.0	.8	.62E-01	.002	.184	0.00000	.00000	.00100	.00006	.00002	0.00000	7.83701	5.83824
72	166.8	2.5619	1385.7	25.7	.4	.32E-01	.001	.194	0.00000	.00000	.00097	.00004	.00001	0.00000	7.86966	6.08091
73	173.0	2.8385	1335.7	26.5	.2	.15E-01	.001	.210	0.00000	.00000	.00095	.00002	.00000	0.00000	7.83532	6.32395
74	179.5	3.1499	1277.7	25.7	.1	.44E-02	.000	.227	0.00000	.00000	.00093	.00001	.00000	0.00000	7.24060	6.21458
75	183.8	3.4909	1217.5	23.7	.0	.12E-02	.000	.241	0.00000	0.00000	.00091	.00001	.00000	0.00000	6.21907	5.76019
76	192.4	3.8814	1157.9	21.2	.0	.24E-03	.000	.253	0.00000	0.00000	.00089	.00000	.00000	0.00000	5.09219	5.14707
77	198.9	4.2818	1102.8	18.7	.0	.41E-04	.000	.265	0.00000	0.00000	.00087	.00000	.00000	0.00000	4.03943	4.50672
78	205.5	4.6957	1052.6	16.7	.0	.67E-05	.000	.274	0.00000	0.00000	.00085	.00000	.00000	0.00000	3.23644	3.95013

TABLE A-3 (cont.)

```
 79 212.2  5.1710 1036.7  15.2       .0  .11E-05   .000 .282 0.00000 0.00000  .00083  .00000  .00000 0.00000 2.60849 3.49672

 80 219.1  5.6974  964.0  14.1       .0  .18E-06   .000 .292 0.00000 0.00000  .00081  .00000 0.00000 0.00000 2.13658 3.13849
SODIUM-D ENERGY  262.535 CAL/G

SODIUM-D LUMINOSITY   43598.07 CD-SEC/G
GRAY BODY LUMINOSITY   6125.40 CD-SEC/G
TOTAL LUMINOSITY      49723.47 CD-SEC/G

TOTAL GRAY BODY ENERGY 2711.676 CAL/G

BAND GRAY BODY ENERGIES
1.5- 2.5   869.287 CAL/G
2.5- 3.5   420.508 CAL/G

  01

                                THERMODYNAMIC EQUILIBRIUM COMBUSTION PROPERTIES AT ASSIGNED

                                                PRESSURES

                                                                                WT FRACTION   ENERGY   STATE   TEMP    DENSITY
        CHEMICAL FORMULA                                                        (SEE NOTE)    CAL/MOL          DEG K   G/CC
FUEL    MG 1.00000                                                               .18175          0.000    S     298.15   1.7400
FUEL    NA 1.00000    N  1.00000   O  3.00000                                    .11791   -111540.000    S     298.15   2.2600
FUEL    C  5.83000    H  8.36000   O  1.15000   N  .30000                        .01420    -53900.000    L     293.15  -0.0000
FUEL    H  8.26000    O  2.00000                                                 .68643          0.000    G     298.15  -0.0000

             O/F= 0.0000    PERCENT FUEL=100.0000    EQUIVALENCE RATIO= 2.4091    REACTANT DENSITY= 0.0000


THERMODYNAMIC PROPERTIES

P, ATM            0.0100
T, DEG K                C
RHO, G/CC      1.0000 E 0
H, CAL/G           -1.1
S, CAL/(G)(K)     1.4400

M, MOL WT         2.000
(DLV/DLP)T     0.00000
(DLV/DLT)P        0.0000
CP, CAL/(G)(K)    0.0000
GAMMA (S)         0.0000
```

subroutine THERMP, and may also be seen in the sample output.

At this point a card with the word "SPECies" may be placed, followed by a card listing up to 9 species (less the number of desired bands) for which mole fractions are to be printed at each point computed.

Before or after the species cards one may place a card with the word "BANDs", followed by a card listing the wavelength bands (in μm) in which it is desired to know the amount of graybody radiation. Up to five bands may be specified. Formats for species and bands cards are given in statements numbered 33 and 54, respectively in subroutine THERMP.

Upon encountering a blank card or a second "CONDitions" card the program proceeds with actual computations. A second blank card here causes the program to exit after the computations are complete. Otherwise more input parameters may be furnished for another calculation using the same formula and percentage amounts, but different burning conditions.